[21] Coban C, Igari Y, Yagi M, Reimer T, Koyama S, Aoshi T, et al. Immunogenicity of whole-parasite vaccines against *Plasmodium falciparum* involves malarial hemozoin and host TLR9. Cell Host Microbe 2010;7(January (1)): 50–61.
[22] Onishi M, Kitano M, Taniguchi K, Homma T, Kobayashi M, Sato A, et al. Hemozoin is a potent adjuvant for hemagglutinin split vaccine without pyrogenicity in ferrets. Vaccine 2014;32(May (25)):3004–9.
[23] Sakabe S, Ozawa M, Takano R, Iwastuki-Horimoto K, Kawaoka Y. Mutations in PA, NP, and HA of a pandemic (H1N1) 2009 influenza virus contribute to its adaptation to mice. Virus Res 2011;158(June (1–2)):124–9.
[24] Yamada S, Hatta M, Staker BL, Watanabe S, Imai M, Shinya K, et al. Biological and structural characterization of a host-adapting amino acid in influenza virus. PLoS Pathog 2010;6(8):e1001034.
[25] Uraki R, Kiso M, Iwatsuki-Horimoto K, Fukuyama S, Takashita E, Ozawa M, et al. A novel bivalent vaccine based on a PB2-knockout influenza virus protects mice from pandemic H1N1 and highly pathogenic H5N1 virus challenges. J Virol 2013;87(July (14)):7874–81.
[26] Kida H, Brown LE, Webster RG. Biological activity of monoclonal antibodies to operationally defined antigenic regions on the hemagglutinin molecule of A/Seal/Massachusetts/1/80 (H7N7) influenza virus. Virology 1982;122(October (1)):38–47.
[27] Das SC, Hatta M, Wilker PR, Myc A, Hamouda T, Neumann G, et al. Nanoemulsion W805EC improves immune responses upon intranasal delivery of an inactivated pandemic H1N1 influenza vaccine. Vaccine 2012;30(November (48)):6871–7.
[28] Jia N, Wang SX, Liu YX, Zhang PH, Zuo SQ, Lin Z, et al. Increased sensitivity for detecting avian influenza-specific antibodies by a modified hemagglutination inhibition assay using horse erythrocytes. J Virol Methods 2008;153(October (1)):43–8.
[29] Kayali G, Setterquist SF, Capuano AW, Myers KP, Gill JS, Gray GC. Testing human sera for antibodies against avian influenza viruses: horse RBC hemagglutination inhibition vs. microneutralization assays. J Clin Virol 2008;43(September (1)):73–8.
[30] Clements ML, Betts RF, Tierney EL, Murphy BR. Serum and nasal wash antibodies associated with resistance to experimental challenge with influenza A wild-type virus. J Clin Microbiol 1986;24(July (1)):157–60.
[31] Benton KA, Misplon JA, Lo CY, Brutkiewicz RR, Prasad SA, Epstein SL. Heterosubtypic immunity to influenza A virus in mice lacking IgA, all Ig, NKT cells, or gamma delta T cells. J Immunol 2001;166(June (12)):7437–45.
[32] Shio MT, Kassa FA, Bellemare MJ, Olivier M. Innate inflammatory response to the malarial pigment hemozoin. Microbes Infect 2010;12(November (12–13)): 889–99.

European Journal of Immunology

# TLR9 and STING agonists synergistically induce innate and adaptive type-II IFN

*Burcu Temizoz[1], Etsushi Kuroda[1], Keiichi Ohata[1], Nao Jounai[2], Koji Ozasa[2], Kouji Kobiyama[2], Taiki Aoshi[2] and Ken J. Ishii[1,2]*

[1] Laboratory of Vaccine Science, WPI Immunology Frontier Research Center (iFReC), Osaka University, Osaka, Japan
[2] Laboratory of Adjuvant Innovation, National Institute of Biomedical Innovation (NIBIO), Osaka, Japan

**Agonists for TLR9 and Stimulator of IFN Gene (STING) act as vaccine adjuvants that induce type-1 immune responses. However, currently available CpG oligodeoxynucleotide (ODN) (K-type) induces IFNs only weakly and STING ligands rather induce type-2 immune responses, limiting their potential therapeutic applications. Here, we show a potent synergism between TLR9 and STING agonists. Together, they make an effective type-1 adjuvant and an anticancer agent. The synergistic effect between CpG ODN (K3) and STING-ligand cyclic GMP–AMP (cGAMP), culminating in NK cell IFN-γ (type-II IFN) production, is due to the concurrent effects of IL-12 and type-I IFNs, which are differentially regulated by IRF3/7, STING, and MyD88. The combination of CpG ODN with cGAMP is a potent type-1 adjuvant, capable of inducing strong $T_h1$-type responses, as demonstrated by enhanced antigen-specific IgG2c and IFN-γ production, as well as cytotoxic $CD8^+$ T-cell responses. In our murine tumor models, intratumoral injection of CpG ODN and cGAMP together reduced tumor size significantly compared with the singular treatments, acting as an antigen-free anticancer agent. Thus, the combination of CpG ODN and a STING ligand may offer therapeutic application as a potent type-II IFN inducer.**

**Keywords:** Adjuvant · cGAMP · CpG ODN · IFN-γ · STING · TLR ·

Additional supporting information may be found in the online version of this article at the publisher's web-site

## Introduction

Pathogen-derived factors, such as LPS or unmethylated CpG DNA (CpG), stimulate innate immune cells to produce cytokines, such as IL-12 and type-I or type-II IFNs, which help generate $T_h1$-type responses and cellular immunity [1, 2]. IL-12 acts on naïve $CD4^+$ T cells to drive $T_h1$ development and IFN-γ production [3, 4]. IFN-γ-producing $T_h1$ cells, in turn, are the main players in the induction of type-1 immunity, which is distinguished by high phagocytic activity [5, 6]. Moreover, $T_h1$ cells play key roles in the generation of antitumor immunity, helping with proper activation and effector functions of CTL, including IFN-γ production [7, 8]. Thus, agents that can induce strong $T_h1$-type responses, CTL, and NK cells [9] are urgently needed, as they may play critical roles in developing efficient vaccine adjuvants or immunotherapeutic agents against intracellular pathogens or cancer.

CpG oligodeoxynucleotides (ODNs) are synthetic single-stranded DNAs containing unmethylated CpG motifs with immunostimulatory properties due to their resemblance to bacterial genomes, and are recognized by TLR9 in certain types of innate immune cells [10, 11]. Upon ligand binding, TLR9 signals through the adaptor molecule MyD88, leading to production of

*Correspondence:* Prof. Ken J. Ishii
e-mail: kenishii@biken.osaka-u.ac.jp

IRF7-dependent type-I IFNs and NF-κB-dependent cytokines [12]. Additionally, in vivo, CpG ODNs have been reported to induce $T_h1$-type responses because of the types of cytokines that are induced by CpG ODNs in APCs [12]. Among the different types of CpG ODNs, D-type CpG ODNs strongly induce both type-I and type-II IFNs, but are not capable of inducing B-cell activation [12, 13]. K-type CpG ODNs (K3 CpG) strongly induce B-cell activation, resulting in IL-6 and antibody production, while they only weakly induce type-I and type-II IFNs [12, 13]. However, since D-type CpG ODNs form aggregates, only K3 CpG is available for clinical use [12, 13].

Along with microbial DNA, host DNA can also become a danger signal, specifically if it inappropriately locates in the cytosol, thereby leading to production of IFNs and proinflammatory cytokines [14, 15]. One recently identified cytosolic DNA sensor is cyclic GMP–AMP (cGAMP) synthase, which catalyzes production of a noncanonical cyclic dinucleotide cGAMP (2′3′cGAMP), containing noncanonical 2′,5′ and 3′,5′ linkages between its purine nucleosides [16]. Canonical cGAMP (3′3′) is synthesized within bacteria and differs from mammalian 2′3′cGAMP in that GMP and AMP nucleosides are joined by bis-(3′,5′) linkages [17, 18].

In addition to cGAMP, c-di-AMP and c-di-GMP, which are cyclic dinucleotides of bacterial origin, are ligands for the adaptor molecule Stimulator of IFN Gene (STING) that signals through the TBK1-IRF3 axis to induce type-I IFN production and NF-κB-mediated cytokine production [19, 20]. Recent studies have shown that these cyclic dinucleotides function as potent vaccine adjuvants due to their ability to enhance antigen-specific T-cell and humoral immune responses [21]. Nevertheless, our group previously demonstrated that a STING ligand, DMXAA, induces type-2 immune responses unexpectedly [22] via STING-IRF3-mediated production of type-I IFNs. As type-2 immune responses often fail to induce type-1 immune responses, the clinical usefulness of STING ligands, including cyclic dinucleotides, was debatable. For example, the most common adjuvant, aluminum salt (alum), lacks the ability to induce cell-mediated immunity, which is considered protective in cases of intracellular pathogen-derived diseases or cancer [23]. To overcome this limitation, alum has been combined with many different kinds of adjuvants, including monophosphoryl lipid A [24] and CpG ODN [25].

Based on the evidence described above, we tried to overcome the issues that K3 CpG and cGAMP possess individually by combining K3 CpG and 3′3′cGAMP. We investigated the immunological characteristics, potency as a vaccine adjuvant and potential as an antitumor immunotherapeutic of this combination, as well as its mechanisms of action in vitro and in vivo. In vitro, the effect of combined K3 CpG and cGAMP was analyzed using human and mouse PBMCs (mPBMCs). Additionally, the effect of this combination was analyzed in vivo via an immunization model by measuring the induction of antigen-specific T- and B-cell responses after combination immunization. Finally, we evaluated the ability of combined K3 CpG and cGAMP to suppress tumor growth in a mouse tumor model. Our results suggest that the combination of K3 CpG and cGAMP makes a potent type-1 adjuvant and a promising immunotherapeutic agent for cancer.

## Results

### Combination of K3 CpG and cGAMP potently induces IFN-γ in human PBMCs (hPBMCs)

K3 CpG is a humanized K-type (also known as B) CpG ODN that has been reported to induce type-1 immune responses, yet only weakly induces IFNs [13, 26]. On the other hand, while cGAMP can induce robust type-I IFNs and acts as an adjuvant [21], other STING ligands were reported to induce type-2 immune responses [22]. To overcome these known limits of K3 CpG and cGAMP, we examined the immunostimulatory properties of a combination of K3 CpG and the canonical 3′3′cGAMP in vitro in hPBMCs. After screening many cytokines using multiple hPBMCs to find interactions between TLR9- and STING-mediated signaling pathways (data not shown), we found that our combination displays potent synergism in the induction of IFN-γ, approximately 10- to 90-fold more than stimulation with K3 CpG or cGAMP alone (Fig. 1A).

Next, to identify the major IFN-γ-producing cell type in hPBMCs, we performed intracellular staining of IFN-γ in hPBMCs stimulated with K3 CpG, cGAMP, or the combination (gating strategy is shown in Supporting Information Fig. 2). Our results indicate that $CD3^-CD56^+CD16^+$ NK cells are the major producers of synergistic IFN-γ among the hPBMCs in response to the combination stimulation, while $CD8^+$ T cells and other cells produced a minimal amount of IFN-γ (Fig. 1B).

Type-I IFNs and IL-12 are capable of activating NK cells for IFN-γ production in addition to inducing type-1 immune responses [27, 28]. Therefore, we next examined the role of IL-12 and type-I IFNs in the combination-induced innate IFN-γ production in hPBMCs. Treatment with IL-12 neutralizing antibody partially reduced the synergistic IFN-γ induction by the combination stimulation (Fig. 1C). Although treatment with type-I IFN neutralizing antibody did not have any effect on the combination-induced IFN-γ production, neutralizing both type-I IFNs and IL-12 at the same time further reduced the synergistic IFN-γ production (Fig. 1C). These results suggest that IL-12 works in coordination with type-I IFNs for the synergistic production of IFN-γ by hPBMCs. Taken together, the results above indicate that, when combined, K3 CpG and cGAMP can be potent NK activators, leading to the production of large amounts of IFN-γ through mechanisms partially dependent on IL-12 and type-I IFNs.

### Cellular and intracellular mechanisms of the synergistic IFN-γ induction by K3 CpG and cGAMP in mice

To examine the synergism between our TLR9 and STING agonists for early (innate) IFN-γ induction in mice, we stimulated mPBMCs in vitro with K3 CpG, cGAMP, or the combination. Large amounts of IFN-γ production were observed in a synergistic manner similar to what we observed in hPBMCs (Fig. 2A). Since IRF3 and IRF7 are the necessary downstream molecules for cGAMP- and CpG-mediated type-I IFN induction, respectively [17, 29], we examined

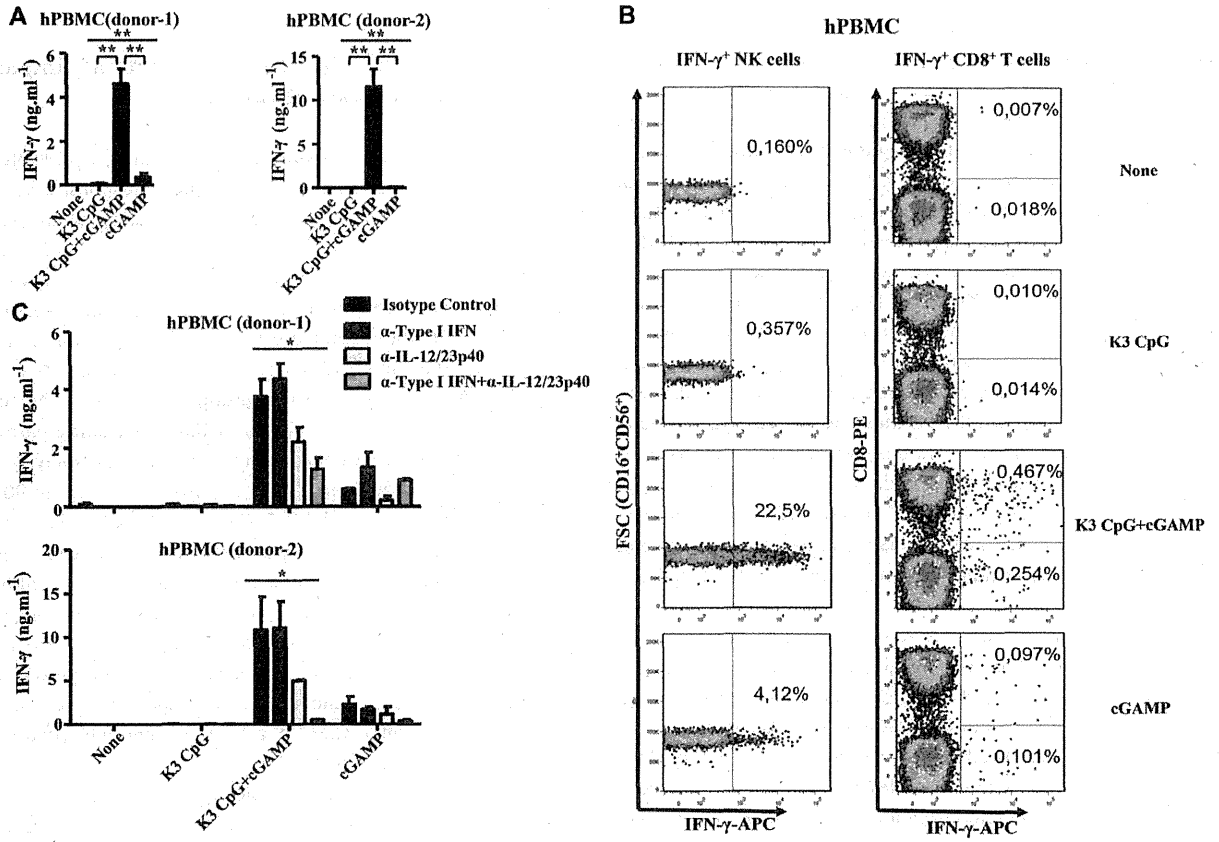


**Figure 1.** K3 CpG and cGAMP (TLR9 and STING agonists, respectively) synergistically induce innate IFN-γ production by human NK cells. (A) hPBMCs from two healthy donors were incubated with K3 CpG (10 μg/mL), cGAMP (10 μM), or K3 CpG (10 μg/mL) + cGAMP (10 μM) for 24 h and the supernatant IFN-γ concentrations were measured by ELISA. Data are representative of at least two independent experiments, and are shown as the mean + SD of duplicates from one experiment, representative of at least two performed. *$p < 0.05$; **$p < 0.01$ (one-way ANOVA with Bonferroni's multiple comparison test). (B) hPBMCs from three healthy donors were stimulated with K3 CpG, cGAMP, or K3 CpG + cGAMP for 16 h, with the last 4 h in the presence of Brefeldin A. After stimulation, cells were analyzed by flow cytometry for the detection of IFN-γ-producing cells. The percentage of IFN-γ-producing $CD3^+CD8^+$ T cells, $CD3^+CD8^-$ T cells (including $CD4^+$ T cells), and $CD3^-CD56^+CD16^+$ NK cells are indicated in the quadrants. Data from one donor, which is representative of three donors, is shown. (C) hPBMCs from two healthy donors were treated with 5 μg/mL of isotype control, type-I IFN neutralizing, IL-12/23p40 neutralizing, or type-I IFN + IL-12/23p40 neutralizing antibodies 30 min prior to 24 h of stimulation with K3 CpG, cGAMP, or K3 CpG + cGAMP. IFN-γ production was measured by ELISA. Data are representative of at least two independent experiments, and are shown as the mean + SD of duplicates from one experiment, representative of at least two performed. *$p < 0.05$; **$p < 0.01$ (one-way ANOVA with Bonferroni's multiple comparison test).

the roles of IRF3 and IRF7 in the synergistic IFN-γ production using mPBMCs derived from either mice deficient for both IRF3 and IRF7 (double knockout, DKO). The synergistic IFN-γ production was abrogated in the IRF3/7 DKO mPBMCs (Fig. 2A).

As IL-12 and type-I IFNs are responsible for the synergistic IFN-γ production in hPBMCs (Fig. 1C), we further examined the ability of combined K3 CpG and cGAMP to activate dendritic cells (DC) that can produce IL-12 and/or type-I IFNs. When we incubated GM-CSF-derived DCs (GM-DCs) and Flt3L-derived DCs (FL-DCs) with K3 CpG, cGAMP, or the combination, we found a similar synergy to the one we observed in mPBMCs (Fig. 2B to D). The combination of K3 CpG and cGAMP induced significantly higher IL-12p40 production by both GM-DCs (Fig. 2B) and FL-DCs (Fig. 2C), and significantly higher IFN-α production by FL-DCs (Fig. 2D) than the amounts induced by singular stimulations. This suggests a potential role for IL-12 and type-I IFNs in the synergistic IFN-γ induction by our combination. Together these results demonstrate that the synergy between K3 CpG and cGAMP that potently induces IFN-γ in hPBMCs was reproduced in mice. The mechanisms for this synergism involve IRF3/7-mediated intracellular signaling, and the synergy induces type-I IFNs by plasmacytoid DCs (pDCs) as well as IL-12 production by both conventional DCs and pDCs.

## TLR9/STING agonists induce type-1 immunity, $CD8^+$ T cells, and suppress type-2 immunity

Given the presence of different kinds of agonistic STING ligands, c-di-GMP, the mammalian 2′3′cGAMP and DMXAA, which was reported to induce type-2 immune responses [18, 19, 22], we

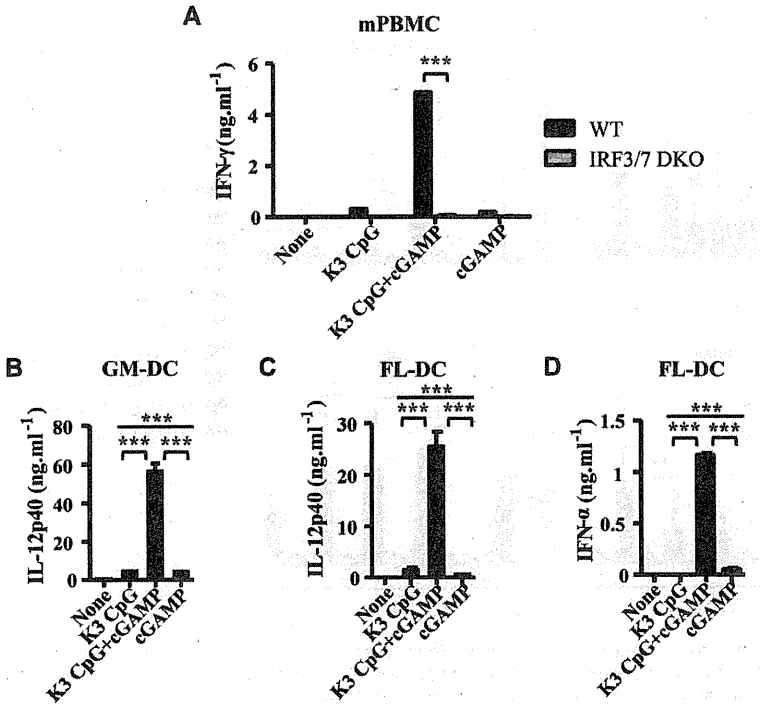


**Figure 2.** Combination of K3 CpG and cGAMP causes synergistic induction of innate IFN-γ in mPBMCs in an IRF3/7-dependent manner and production of IFN-α and IL-12 by DCs. (A) mPBMCs from WT and IRF3/7 DKO mice were stimulated with K3 CpG, cGAMP, or K3 CpG + cGAMP for 24 h and IFN-γ production was measured by ELISA. Data are representative of two independent experiments, and are shown as the mean + SEM of duplicates from one experiment, representative of two performed. ***$p < 0.001$ (Student's *t*-test); (B) GM-DCs were stimulated with K3 CpG, cGAMP, or K3 CpG + cGAMP for 24 h, and IL-12p40 production was measured by ELISA. (C and D) FL-DCs were stimulated with K3 CpG, cGAMP, or K3 CpG + cGAMP for 24 h, and (C) IL-12p40 and (D) IFN-α production were measured by ELISA. (B to D) Data are representative of two independent experiments and are shown as the mean + SD of duplicates from one experiment, representative of two performed. ***$p < 0.001$ (one-way ANOVA with Bonferroni's multiple comparison test).

next examined the ability of K3 CpG to synergize with these other STING ligands. mPBMCs stimulated with not only 3′3′cGAMP, but also 2′3′cGAMP and c-di-GMP synergized with K3 CpG to induce innate IFN-γ production (Fig. 3A).

To evaluate the adjuvant properties of these combinations in vivo, we immunized mice with the OVA protein and K3 CpG, STING agonists, or combinations of K3 CpG and STING agonists twice, at days 0 and 10. At day 17, antigen-specific antibody responses and spleen cell responses were examined. All mouse groups adjuvanted with STING agonists, such as cGAMP, c-di-GMP, and DMXAA, but not those adjuvanted with the TLR9 agonist, K3 CpG, had type-2 immune responses characterized by a high titer of serum anti-OVA IgG1 (Fig. 3B), and OVA-specific IL-13 production by splenocytes (Fig. 3C). By sharp contrast, the addition of K3 CpG converted all of the type-2 immune responses induced by STING agonists into type-1 immune responses, characterized by strong induction of OVA-specific serum IgG2c and splenocyte IFN-γ, while shutting down OVA-specific IgG1 and IL-13 production (Fig. 3B and C). We also observed synergistic induction of IFN-γ by OVA-specific $CD8^+$ T cells (Supporting Information Fig 1A). Furthermore, our in vivo CTL cytotoxicity assay (gating strategy is shown in Supporting Information Fig. 3) revealed that compared to the PBS, K3 CpG, or cGAMP immunization groups, combination of K3 CpG and cGAMP could induce strong antigen-specific $CD8^+$ CTL cytotoxicity (Supporting Information Fig. 1B) These results suggest that combinations of TLR9 and STING agonists result in potent type-1 adjuvants, capable of inducing robust $CD8^+$ T-cell responses, in addition to the induction of synergistic adaptive IFN-γ production in the antigen-stimulated spleen cells of the combination-immunized mice, and of suppressing the type-2 immune responses that are induced by STING ligands.

## Synergistic induction of IFN-γ depends on IRF3/7, STING, MyD88, IL-12, and type-I IFN signaling

We showed in mPBMCs that synergistic production of innate IFN-γ was completely dependent on IRF3 and IRF7, which are required for the induction of type-I IFNs by cGAMP and K3 CpG, respectively. Since cGAMP is a ligand for STING, and K3 CpG is a ligand for TLR9 that signals via the adapter molecule MyD88, we evaluated the involvement of IRF3/7, MyD88, STING, and type-I IFNs in the combination-induced synergistic production of antigen-specific IFN-γ, using IRF3/7 DKO, IFN-α/β receptor (IFNAR) KO, MyD88 KO, and STING mutant mice. Combination-induced antigen-specific IgG2c in the sera and IFN-γ production by spleen were significantly decreased in the STING mutant, IRF3/7 DKO, MyD88 KO, and IFNAR KO mice, compared with the WT mice (Fig. 4A and B).

Our in vitro studies in mouse and hPBMCs also showed that IL-12 contributes to synergistic induction of innate IFN-γ. Therefore, we next investigated the involvement of IL-12 by using IL-12p40$^{+/-}$ and IL-12p40$^{-/-}$ mice. We found that IL-12p40 was required for the synergistic induction of antigen-specific IFN-γ, but not for the induction of IgG2c antibody responses (Fig. 4C and D). Overall our results suggest that the combination of K3 CpG and cGAMP is a potent type-1 adjuvant, synergistically inducing the production of antigen-specific IFN-γ in an IRF3/7, STING, MyD88, IL-12, and type-I IFN signaling-dependent manner.

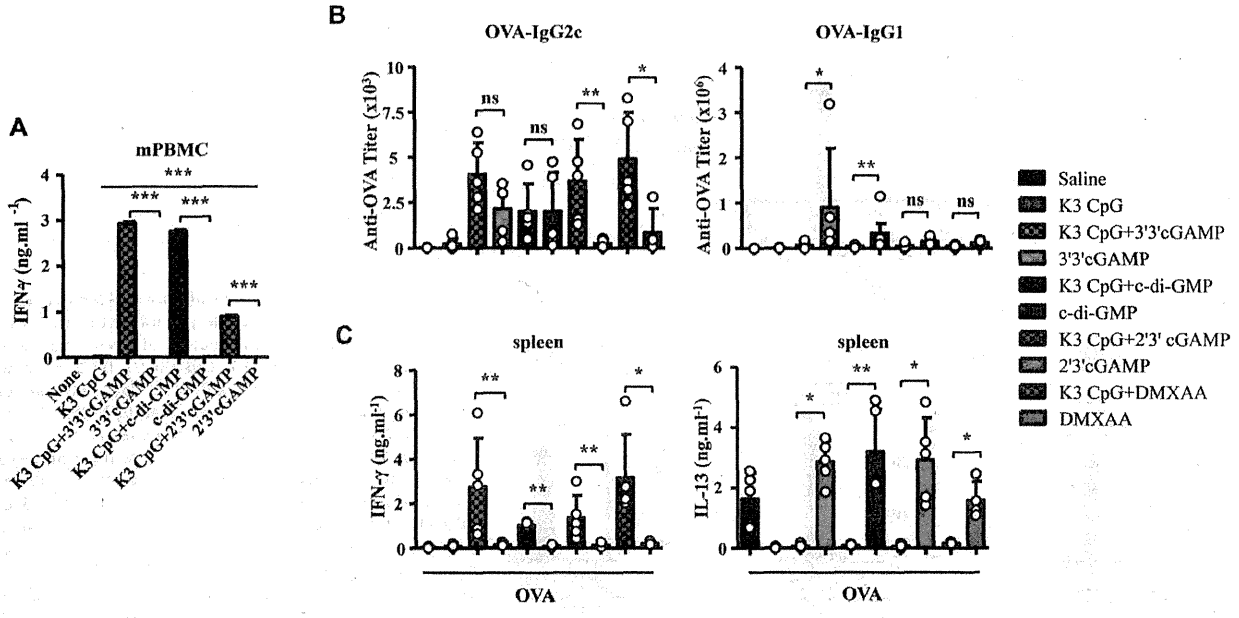


**Figure 3.** Combinations of TLR9 and STING agonists are potent type-1 adjuvants that also suppress type-2 immune responses in vivo. (A) mPBMCs were stimulated with K3 CpG (10 μg/mL), STING agonists (10 μM), or K3 CpG + STING agonists for 24 h and IFN-γ production was measured by ELISA. Data are representative of two independent experiments, and are shown as the mean + SEM of duplicates from one experiment, representative of two performed.*$p < 0.05$; **$p < 0.01$; ***$p < 0.001$ (one-way ANOVA with Bonferroni's multiple comparison test). (B and C) Mice ($n \geq 4$) were immunized i.m. with OVA (10 μg) with or without K3 CpG (10 μg), 3′3′/2′3′cGAMP (1 μg), c-di-GMP (1 μg), DMXAA (50 μg), or K3 + 3′3′/2′3′cGAMP/c-di-GMP/ DMXAA at days 0 and 10. (B) On day 17, OVA-specific serum IgG1 and IgG2c were measured by ELISA. (C) Spleen cells were stimulated with OVA (10 μg/mL) protein for 48 h. Production of IFN-γ and IL-13 were measured by ELISA. (B and C) Each symbol represents an individual mouse. Data are representative of two independent experiments and are shown as the mean + SD of biological replicates from one experiment, representative of two performed. *$p < 0.05$; **$p < 0.01$ (Mann–Whitney U-test).

### Combination of K3 CpG and cGAMP efficiently suppresses tumor growth in a murine model

Because $T_h1$ and $CD8^+$ T-cell responses are important for the generation of antitumor immunity, we investigated the immunotherapeutic potential of the K3 CpG and cGAMP combination in a mouse tumor model. We inoculated mice with OVA-expressing EG-7 lymphoma cells by s.c. injection. On days 7 and 10, mice were given intratumor injections of PBS, K3 CpG (10 μg), cGAMP (10 μg), or K3 CpG and cGAMP. Combination treatment significantly suppressed the tumor growth compared with PBS, K3 CpG, or cGAMP treatments (Fig. 5A), suggesting that our combination can work as an antigen-free immunotherapeutic agent for cancer. In addition, the antitumor effect of the combination, in the EG-7 tumor model, was dependent on the $CD8^+$ T-cell activity, rather than the NK-cell activity, as the combination failed to suppress the tumor growth in the RAG2 KO mice (Supporting information Fig. 4B), and significantly higher amounts of IFN-γ were produced only by the OVA-specific $CD8^+$ T cells of the mice that were treated with the combination (Supporting Information Fig. 4A).

To investigate the antitumor effect of our combination in a tumor model that does not express an artificial antigen, such as OVA, we inoculated mice with B16 F10 melanoma cells that were shown to rely on NK cells for clearance [30] by s.c. injection. On days 8, 11, and 13, mice were given intratumor injections of PBS, K3 CpG (10 μg), cGAMP (10 μg), or K3 CpG and cGAMP. Although cGAMP showed a significant antitumor effect compared to the PBS treatment group, antitumor effect of the combination was the strongest among all groups (Fig. 5B).

## Discussion

Efficient vaccines against intracellular pathogens or cancer require adjuvants that induce type-1 immune responses. Cyclic dinucleotides, such as cGAMP and c-di-GMP, have attracted attention as potential vaccine adjuvants because they directly bind to the transmembrane molecule STING and activate the TBK1-IRF3-dependent signaling pathway to induce type-I IFNs [31]. However, evidence that STING agonists induce type-2 immune responses [22], rather than protective type-1 immune responses, suggests that their potential therapeutic applications are limited. In this study, we solve this issue by combining STING-agonists with K3 CpG, a TLR9 ligand. This combination synergistically enhances innate and adaptive IFN-γ production. It acts as a potent type-1 adjuvant, strongly inducing antibody responses, and $CD4^+$ $T_h1$ and $CD8^+$ T cells, and as an antitumor agent that can efficiently suppress tumor growth in mouse tumor models of lymphoma and melanoma.

The current study demonstrates that the combination of K3 CpG and cGAMP synergistically induces innate IFN-γ production in both human and mPBMCs (Figs. 1 and 2), suggesting that this

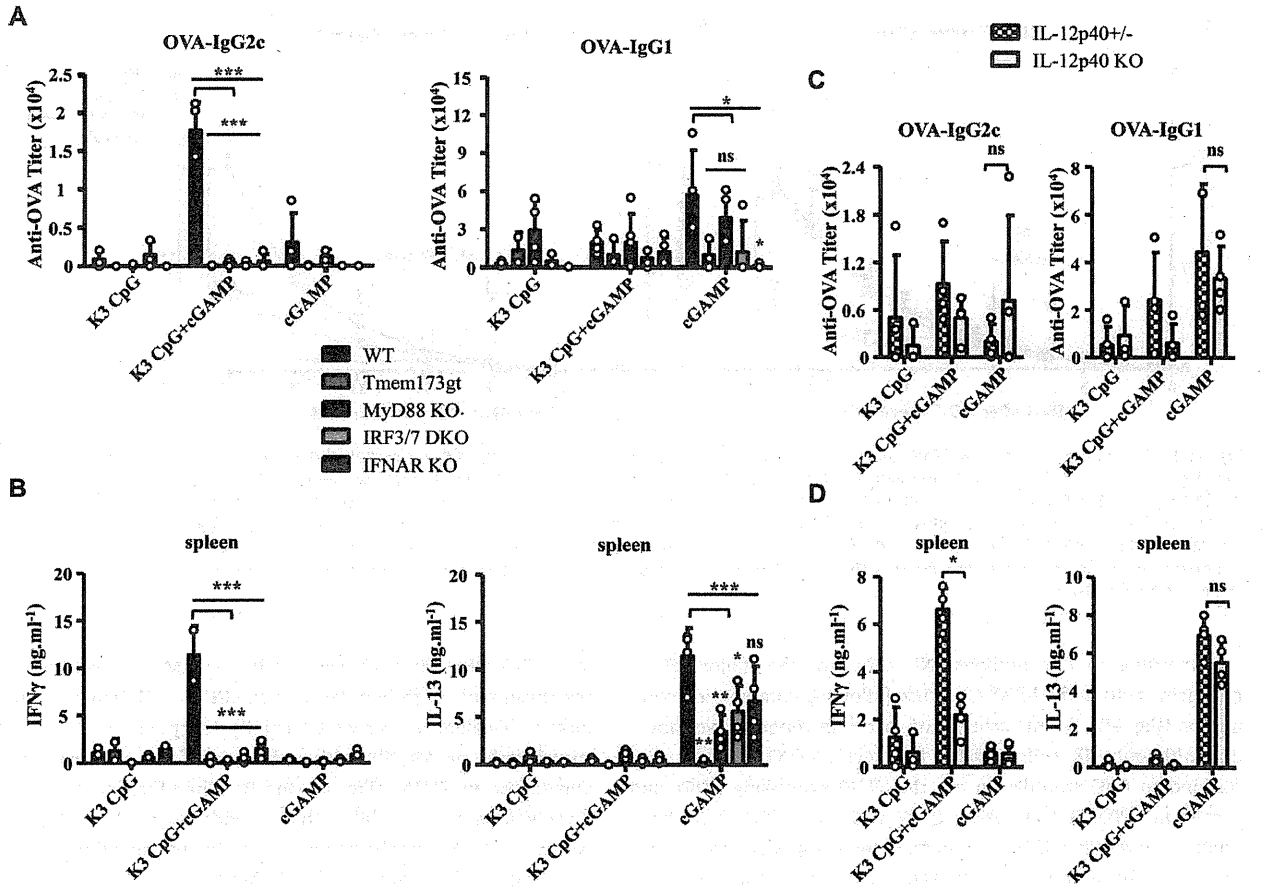


**Figure 4.** The synergistic effect of the combination of K3 CpG and cGAMP on antigen-specific IFN-γ induction is dependent on IRF3/7, STING, MyD88, IL-12, and type-I IFN signaling. (A) WT, Tmem173gt, IRF3/7 DKO, MyD88 KO, and IFNAR KO C57BL/6J mice ($n \geq 3$) were immunized with OVA and K3 CpG, cGAMP, or K3 + cGAMP at days 0 and 10, via the i.m. route. On day 17, OVA-specific serum IgG2c and IgG1 were measured by ELISA. Each symbols represent an individual mouse and data are representative of two independent experiments and are shown as the mean + SD of biological replicates from one experiment, representative of two performed. *$p < 0.05$; **$p < 0.01$; ***$p < 0.001$ (one-way ANOVA with Bonferroni's multiple comparison test). (B) Spleen cells from immunized mice were stimulated with OVA for 48 h. Production of IFN-γ and IL-13 were measured by ELISA. Data are representative of two independent experiments and are shown as the mean + SD of biological replicates from one experiment, representative of two performed. *$p < 0.05$; **$p < 0.01$; ***$p < 0.001$ (one-way ANOVA with Bonferroni's multiple comparison test). (C) IL-12p40 +/− and −/− C57BL/6J mice were immunized with OVA and K3 CpG, cGAMP, or K3 CpG + cGAMP at days 0 and 10, via the i.m. route. On day 17, OVA-specific serum IgG2c and IgG1 were measured by ELISA. Data are representative of two independent experiments and are shown as the mean + SD of biological replicates from one experiment, representative of two performed. *$p < 0.05$ (Mann–Whitney U-test). (D) Spleen cells were stimulated with OVA protein for 48 h. Production of IFN-γ was measured by ELISA. Data are representative of two independent experiments and are shown as the mean + SD of biological replicates from one experiment, representative of two performed. *$p < 0.05$ (Mann–Whitney U-test).

phenomenon is conserved between human and mouse. Importantly, combination stimulation does not affect cell viability (Supporting Information Fig. 5), which may affect cytokine production. Our in vitro results also demonstrate that the mechanisms of action involve IL-12 and type-I IFNs. Specifically, during the synergism between K3 CpG and cGAMP, type-I IFNs were dispensable since the loss of their effect can be compensated by the increased production of IL-12 (Fig. 1C and Supporting Information Fig. 6B). A previous report suggested that type-I IFNs and IL-12 can synergistically induce IFN-γ production by $CD4^+$ T cells after Listeria monocytogenes infection. They showed that the synergy was significantly decreased in the absence of both cytokines, but partially decreased in the absence of either one of the cytokines, which is consistent with our results [32]. Moreover, we found that, similar to the synergy observed in PBMCs, our combination can synergistically induce IL-12p40 production in GM-DCs and FL-DCs (Fig. 2C and D), suggesting a potential role for conventional and plasmacytoid DCs in the combination-induced synergy. A similar IL-12 synergy was reported by Krummen et al. by the combination of TLR ligands, CpG and Poly I:C, in BM-derived DCs that required the combination of MyD88- and TRIF-dependent signaling pathways [33]. Our results also demonstrate that the combination of molecules activating MyD88-dependent (TLR9) and independent (STING) signaling pathways results in a robust immunostimulatory agent, suggesting that such combinations might be useful for immunotherapeutic applications.

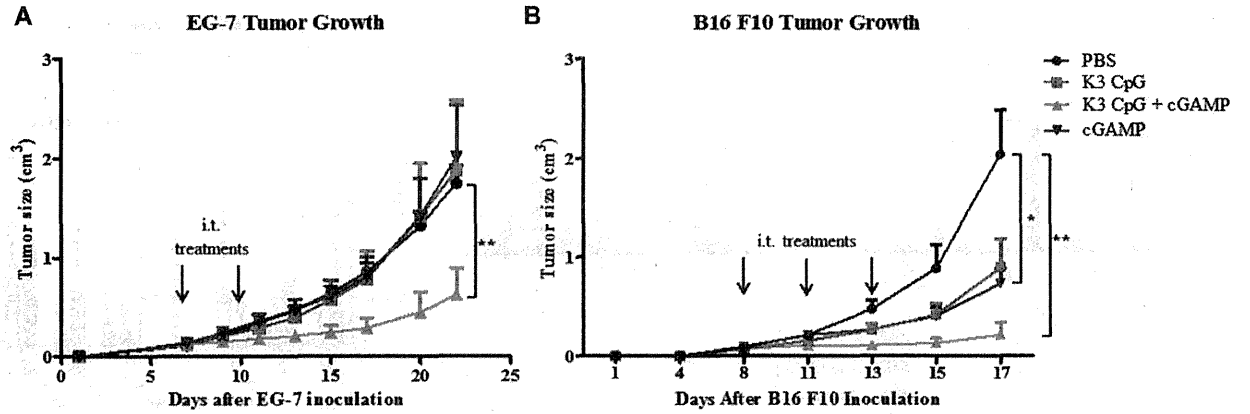


**Figure 5.** The combination of K3 CpG and cGAMP efficiently suppresses tumors in the EG-7 and B16 F10 mouse tumor models. (A) Mice were injected with 1 × $10^6$ EG-7 lymphoma cells (in 100 μL of PBS) s.c. on day 0. On days 7 and 10, mice were given intratumor injections of PBS ($n$ = 8), K3 CpG ($n$ = 8), cGAMP ($n$ = 8), or K3 CpG + cGAMP ($n$ = 9), and were monitored for tumor growth for 22 days. (B) Mice were injected with 0.5 × $10^6$ B16 F10 cells (in 100 μL of PBS) s.c. on day 0. On days 8, 11, and 13, mice were given intratumor injections of PBS ($n$ = 8), K3 CpG ($n$ = 8), cGAMP ($n$ = 8), or K3 CpG + cGAMP ($n$ = 8), and mice were monitored for tumor growth for 17 days. Data are representative of two independent experiments and are shown as the mean + SEM of biological replicates from one experiment, representative of two performed. *$p$ < 0.05; **$p$ < 0.01 (Mann–Whitney $U$-test).

According to our findings, NK cells are the major IFN-γ-producing cells in the hPBMC culture following combination stimulation (Fig. 1B). On the other hand, previous reports have shown that although NK cells express low levels of TLR9, cells that respond to CpG stimulation are the TLR9-expressing pDCs and B cells in hPBMCs [34]. Also, IL-12 and type-I IFNs have been reported to regulate IFN-γ production and cytotoxicity in NK cells [28, 35]. Given those reports and our in vitro data, our proposed mechanism for the synergistic induction of innate IFN-γ is that mainly pDCs may respond to K3 CpG, while, together with pDCs, other cells, such as conventional DCs or macrophages, may respond to cGAMP to produce high amounts of type-I IFNs and IL-12, which then synergize to induce IFN-γ production in NK cells, by signaling through IL-12 and type-I IFN receptors (Supporting Information Fig. 6A).

The first report about the adjuvant effect of 2′3′cGAMP showed that i.m. cGAMP immunization can induce antigen-specific B- and T-cell responses in a STING-dependent manner [21]. Our in vivo immunization studies using 3′3′cGAMP are also consistent with the previous reports; it induces strong antigen-specific B- and T-cell responses in a STING-dependent manner (Fig. 4A and B). We also showed that 3′3′cGAMP is a type-2 adjuvant that can induce not only IgG1, but also IgG2c antibody responses and $T_h2$-type cytokine responses in spleen cells (Fig. 3B and C). Although type-2 adjuvants do not usually induce the production of $T_h1$-like Ig isotype (IgG2c), cGAMP can do so, probably due to its ability to induce type-I IFNs, since type-I IFNs induce IgG2c antibody responses [36]. Moreover, we found that distinct mechanisms were involved in the induction of B- and T-cell responses by cGAMP, in which cGAMP-induced antibody responses, but not $T_h2$ responses, were dependent on type-I IFN signaling (Fig. 4B). In addition, because cGAMP is known to signal only through the STING-IRF3 axis to induce type-I IFN production [17], we expected to observe the loss of antibody and T-cell responses in IRF3/7 DKO mice. However, while cGAMP-induced antibody responses were slightly reduced in the IRF3/7 DKO mice, cGAMP-induced T-cell responses were partially dependent on IRF3/7 and, surprisingly, on MyD88, although such effects were completely dependent on STING (Fig. 4A and B). Therefore, we are further investigating the possibility that in addition to the STING-IRF3 pathway, cGAMP might activate an unknown signaling pathway that involves the adapter molecule MyD88.

Although K3 CpG was reported as an adjuvant capable of inducing type-1 immune responses [37], we found that K3 CpG by itself was a weak type-1 adjuvant, as it failed to induce antigen-specific antibody or T-cell responses at levels comparable with the cGAMP or combination immunization groups (Fig. 3B and C). Interestingly, the combination of a weak type-1 adjuvant, K3 CpG, with a type-2 adjuvant, cGAMP, resulted in a strong type-1 adjuvant that induced synergistic antigen-specific IFN-γ production and strong $T_h1$-like antibody and $CD8^+$ T-cell responses (Fig. 3 and Supporting Information Fig. 1). Our findings are also consistent with a previous study showing that the combination of CpG and IFA, a type-2 adjuvant, induces type-1 immune responses while suppressing type-2 immune responses [37]. Importantly, in addition to the induction of potent type-1 immune responses by our combination, we showed that it can also suppress the type-2 responses that are induced by cGAMP that is important for increased safety as dominant type-2 responses have been reported to cause a number of chronic diseases, such as allergy [5, 38, 39]. Our results are also consistent with the findings of Lin et al., in that production of IgG2c was enhanced while the production of IgG1 was suppressed by CpG [40]. Furthermore, the synergistic effect of our combination on antigen-specific IFN-γ induction is dependent on IRF3 and IRF7 (Fig. 4A and B), indicating that type-I IFNs may also play an important role in this synergy. This idea is further supported by the complete abolishment of synergy that we observed in IFNAR KO mice (Fig. 4A and B). Moreover, because MyD88 is a

downstream signaling molecule of TLR9 and cGAMP is a ligand of STING, we found that the type-1 immunity-inducing effect of the combination is dependent on both MyD88 and STING, as expected (Fig. 4A and B). On the other hand, we showed that IL-12p40 is required for the synergistic induction of $T_h1$-type cytokine responses, but not for the induction of IgG2c antibody responses (Fig. 4C and D). Because IL-12 is important for $T_h1$-cell development and IFN-γ production [3, 4], it is reasonable to observe IL-12 dependency in the $T_h1$-type cytokine responses. A possible explanation for the IL-12-independent IgG2c induction by our combination could be that production of type-I IFNs in the KO mice might be compensating for the absence of IL-12. Previous reports showed that type-I IFNs can induce IgG2c antibody responses in a T-cell-independent manner [36], while IL-12 induces IgG2c antibody responses by inducing IFN-γ production from T or NK cells [41]. In addition, use of anti-IL-12/23p40 neutralizing antibodies in our in vitro studies and IL-12p40 mice in the in vivo studies cannot rule out the possible involvement of IL-23 in the mechanisms of innate or adaptive IFN-γ synergy, as IL-23 signaling, which was shown to affect NK-cell activation and T-cell responses [42, 43], will be defective in both experimental designs. Our studies regarding this issue showed that although no antigen-specific IL-17 was detected in the spleen cell cultures of the immunized mice as an indirect indicator of in vivo IL-23 induction, and no IL-23 was induced in mPBMCs by combination stimulation, IL-23 is induced in the FL-DCs only by combination stimulation, but not by cGAMP or K3 CpG stimulations (data not shown), suggesting a possible role for IL-23 in the mechanisms of innate or adaptive IFN-γ synergy, which needs further investigation.

Finally, we found the K3 CpG and cGAMP combination has a strong antitumor effect, as only treatment with the combination could efficiently suppressed tumor growth in the EG-7 mouse tumor model (Fig. 5A). Because our in vivo results show that the combination induces strong $CD8^+$ T-cell responses (Supporting Information Fig. 1A and B), and the antitumor effect of the combination is lost in the RAG2 KO mice (Supporting Information Fig. 4B), which lacks $CD8^+$ T cells, we concluded that the antitumor effect of our combination is due to the induction of robust $CD8^+$ cytotoxic T-cell activation. Our hypothesis is supported by a previous report showing that vaccination with OVA-conjugated CpG ODN also has potent antitumor effects, which are dependent on $CD8^+$ T cells [44]. Moreover, since we identified NK cells as the main players in the IFN-γ synergy in our in vitro hPBMC studies, we also investigated the antitumor effect of our combination in the B16 F10 mouse melanoma tumor model, which relies on NK cells for clearance [30] and does not express artificial antigens. Although cGAMP, itself, could significantly suppress the tumor growth compared to the control group, combination had the strongest antitumor effect, resulting in almost complete tumor elimination (Fig. 5B). Thus, our combination is a strong antitumor agent, capable of suppressing tumors that relies not only on $CD8^+$ T cells, but also on NK cells for clearance. Furthermore, the advantage of our combination therapy over previously reported CpG-based antitumor agents, such as OVA-conjugated CpG ODN [44] or nanoparticle-conjugated CpG ODN [45], is that it does not require a chemical conjugation between K3 CpG and cGAMP. Additionally, unlike those systems, our approach does not require the injection or conjugation of a tumor antigen. It works as an antigen-free antitumor agent rather than a preventive vaccine.

In conclusion, our study suggests that combination of TLR9 and STING agonists is an advantageous type-1 adjuvant for vaccines requiring strong cellular immune responses, and a promising antitumor agent that can also stimulate human NK cells for synergistic IFN-γ production. Thus, our results provide insight into the mechanisms of the combined action of TLR9 and STING signaling pathways, which potentially promote the immunotherapeutic and adjuvant properties of our combination.

## Materials and methods

### Mice

Seven- to ten-week-old female C57BL/6J mice were purchased from CLEA Japan, Inc. (Osaka, Japan). MyD88 KO mice were purchased from Oriental BioService, Inc. (Kyoto, Japan). IL-12p40 KO and STING mutant mice (Tmem173gt), which have a loss-of-function mutation at the ligand-binding site of STING [46], were purchased from Jackson Laboratories (Bar Harbor, ME, USA). IRF3/7 DKO mice were generated from IRF3 KO [22] and IRF7 KO mice, the latter of which was provided by the RIKEN BRC (Ibaraki, Japan) via the National Bio-Resource Project of the MEXT, Japan [47]. IFNAR2 KO mice were obtained from B&K Universal. All of the animal experiments were conducted according to the guidelines of the Animal Care and Use Committee of RIMD and IFReC of Osaka University, and the use of animals was approved by Osaka University.

### Reagents

The 2′3′ and 3′3′ cGAMPs were purchased from Invivogen (San Diego, CA, USA). DMXAA was purchased from Sigma-Aldrich (St. Louis, MO, USA) and dissolved in 5% $NaHCO_3$. Yamasa (Chiba, Japan) kindly donated c-di-GMP. OVA was purchased from Kanto Chemical (Osaka, Japan) and the endotoxin levels were determined by Toxicolor® (Seikagaku Corp., Tokyo, Japan) as less than 1 EU/mg. K3 CpG ODN was synthesized by GeneDesign as previously described [48]. CFSE was purchased from Life Technologies (Carlsbad, CA, USA).

### Immunizations and spleen cell cultures

After anesthetization, C57BL/6J mice were i.m. immunized with OVA (10 μg), or OVA and K3 CpG (10 μg), DMXAA (50 μg), c-di-GMP (1 μg), 2′3′ or 3′3′ cGAMP (1 μg), or K3 CpG + 2′3′/3′3′cGAMP/c-di-GMP/DMXAA at days 0 and 10. On day 17, OVA-specific serum IgG1 and IgG2c were measured by ELISA as

previously described [49]. The secondary antibodies used in IgG2c and IgG1 ELISAs were horseradish peroxidase conjugated goat anti-mouse IgG2c and IgG1 (Bethyl Laboratories, Montgomery, TX). On day 17, spleen cells were collected and single cell suspensions were prepared using a gentleMACS dissociator (Miltenyi Biotech, Gladbach, Germany). After red blood cell lysis using Tris-$NH_4Cl$ buffer, cells were cultured in RPMI (containing 1% penicillin/streptomycin and 10% fetal calf serum [FCS)] and stimulated with total OVA (10 μg/mL) or OVA peptides (10 μg/mL) that are specific for MHC class I (OVA 257) or MHC class II (OVA 323) for 48 h. Production of IFN-γ and IL-13 were measured by ELISA.

## hPBMC isolation and stimulation

All hPBMC experiments were conducted following approval from the Institutional Review Board of the National Institute of Biomedical Innovation. hPBMCs were isolated from the blood of healthy volunteer blood donors, using human lymphocyte separation medium (IBL, Japan), and 1 × $10^6$ cells were cultured in RPMI. PBMCs were stimulated with K3 CpG (10 μg/mL), cGAMP (10 μM), or K3 CpG + cGAMP for 24 h and production of IFN-γ and IL-12 were measured by ELISA.

For in vitro neutralization experiments, hPBMCs that were cultured as described above were subjected to IL-12/23p40 (clone: C8.6, BioLegend, San Diego, CA, USA), type-I IFN (clone: MMHAR-2, PBL Interferon Source, Piscataway, NJ, USA), or both IL-12/23p40 and type-I IFN neutralizing antibody treatments (5 μg/mL) 30 min before 24 h of stimulation.

## mPBMC and DC cultures

mPBMCs were isolated from C57BL/6J mice using mouse lymphocyte separation medium (IBL, Japan), and 0.5 × $10^6$ cells were cultured in RPMI. GM-DC cultures were prepared by flushing BM cells from the tibia and femurs of C57BL/6J mice and culturing these cells for 7 days in the presence of 20 ng/mL of GM-CSF (PeproTech, Rocky Hill, NJ, USA). GM-DCs were cultured in RPMI, containing 1% penicillin/streptomycin and 20% FCS. FL-DC cultures were prepared from BM cells of C57BL/6J mice that were cultured for 7 days in the presence of 100 ng/mL of human Flt3L (PeproTech). FL-DCs were cultured in RPMI, containing 1% penicillin/streptomycin and 10% FCS.

## In vitro cytotoxicity assay

Splenocytes were isolated from C57BL/6J mice and 1 × $10^6$ cells were cultured in RPMI in 96-well round-bottom plates for 24 h with the stimulants. After the stimulation, in order to prepare a positive control, Triton X-100 was added into the nonstimulated cells that were incubated at 37°C for 15 min. After centrifugation, supernatants of the cells were mixed with the substrate mix and incubated for 15 min at room temperature. ODs at 490 nm were measured and the percent cytotoxicity was calculated according to the instructions of the Non-Radioactive Cytotoxicity Assay Kit (Promega, WI, USA).

## Cytokine measurement

Mouse IL-12p40, mouse IL-13, human IFN-γ, and human IL-12 levels were measured using ELISA kits from R&D Systems (Minneapolis, MN, USA). Mouse IFN-γ levels were determined using an ELISA kit from BioLegend.

## Staining for intracellular cytokine and cell surface molecules

hPBMCs were stimulated with K3 CpG (10 μg/mL), cGAMP (10 μM), or K3 CpG + cGAMP for 16 h, with the last 4 h being in the presence of Brefeldin A. After the stimulation, cells were harvested and stained for surface molecules with CD16-PerCP-Cy5.5 (BD Biosciences, Franklin Lake, NJ), CD56-BV421 (BioLegend), CD3-FITC (BD Biosciences), and CD8-PE (Miltenyi Biotech) antibodies. Fixed and permeabilized cells were stained with IFN-γ-allophycocyanin (BioLegend) for the detection of intracellular IFN-γ and analyzed using the BD FACSCANTO II flow cytometer.

## In vivo CTL cytotoxicity assay

Six-week-old C57BL/6J mice were immunized with OVA (10 μg) only, or OVA and either K3 CpG (10 μg), cGAMP (1 μg), or K3 + cGAMP once, via the i.m. route. On day 7, splenocytes from the naïve C57BL/6J mice were labeled with 2 or 0.2 μM of CFSE for 10 min at 37°C. The cells, which were labeled with 2 μM of CFSE, were subjected to peptide pulsing by incubating them with the OVA257 (10 μg/mL) for 90 min at 37°C. Then, the cells were washed, and equal numbers from each cells were transferred to the immunized mice via the i.v. route. Splenocytes were isolated, and upon staining with the LIVE/DEAD® Fixable Near-IR Dead Cell Stain (Invitrogen, Carlsbad, CA, USA), CFSE-labeled cells were analyzed by flow cytometry 24 h after the transfer.

## Tumor cells and treatment

EG-7-OVA thymoma cells were purchased from American Type Culture Collection (VA, USA) and cultured in RPMI. A total of 1 × $10^6$ cells were s.c. injected to the back of mice on day 0. On days 7 and 10, mice were given intratumor injections of PBS (50 μL), K3 CpG (10 μg), cGAMP (10 μg), or K3 CpG + cGAMP, and mice were monitored for tumor growth for 22 days.

B16 F10 melanoma cells were purchased from RIKEN Cell Bank (Japan) and cultured in DMEM. A total of 0.5 × $10^6$ cells were s.c. injected to the back of mice on day 0. On days 8, 11, and 13, mice

were given intratumor injections of PBS (50 μL), K3 CpG (10 μg), cGAMP (10 μg), or K3 CpG + cGAMP, and mice were monitored for tumor growth for 17 days.

### Statistical analysis

Mann–Whitney *U*-test, Student's *t*-test, or one-way ANOVA with Bonferroni's multiple comparison test were used for the statistical analyses ($*p < 0.05$; $**p < 0.01$; $***p < 0.001$). Statistical analyses were performed using GraphPad Prism software (La Jolla, CA, USA).

**Acknowledgments:** We thank Dr. Cevayir Coban for her comments and critical reading of the manuscript. We also thank the staff of the Animal Resource Center for Infectious Diseases (IFReC and RIMD, Osaka University) for their support in these studies and Prof. Akira's group for providing us the use of their flow cytometer. This study was supported in part by the Adjuvant Database Grant. E.K. received a grant-in aid for scientific research from the Ministry of Education, Culture, Sports, Science and Technology (MEXT) of Japan (grant number 24591145) and Takeda Science Foundation. E.K. was also supported by the Regional Strategy Support Program. B.T. received support in the form of a Japanese Government Scholarship from MEXT.

**Conflict of interest:** The authors declare no commercial or financial conflict of interest.

## References

1 **Kawai, T. and Akira, S.**, Review Toll-like receptors and their crosstalk with other innate receptors in infection and immunity. *Immunity* 2011. **34**: 637–650.

2 **Trinchieri, G. and Sher, A.**, Cooperation of Toll-like receptor signals in innate immune defence. *Nat. Rev. Immunol.* 2007. **7**: 179–190.

3 **Seder, R. A., Gazzinelli, R., Sher, A. and Paul, W. E.**, Interleukin 12 acts directly on CD4+ T cells to enhance priming for interferon gamma production and diminishes interleukin 4 inhibition of such priming. *Proc. Natl. Acad. Sci. USA* 1993. **90**: 10188–10192.

4 **Hsieh, C., Macatonia, S. E., Tripp, C. S., Wolf S. F., Garra A. O. and Murphy, K. M.**, Development of TH1 CD4+ T cells through IL-1 2 produced by Listeria-induced macrophages. *Science* 1993. **260**: 547–549.

5 **Spellberg, B. and Edwards, J. E.**, Type 1/type 2 immunity in infectious diseases. *Clin. Infect. Dis.* 2001. **90509**: 76–102.

6 **Mantovani, A. and Sica, A.**, Macrophages, innate immunity and cancer: balance, tolerance, and diversity. *Curr. Opin. Immunol.* 2010. **22**: 231–237.

7 **Hung, K., Hayashi, R., Lafond-Walker, A., Lowenstein, C., Pardoll, D. and Levitsky, H.**, The central role of CD4+ T cells in the antitumor immune response. *J. Exp. Med.* 1998. **188**: 2357–2368.

8 **Vesely, M. D., Kershaw, M. H., Schreiber, R. D. and Smyth, M. J.**, Natural innate and adaptive immunity to cancer. *Annu. Rev. Immunol.* 2011. **29**: 235–271.

9 **Vitale, M., Cantoni, C. and Pietra, G., Mingari, M. C. and Moretta, L.**, Effect of tumor cells and tumor microenvironment on NK-cell function. *Eur. J. Immunol.* 2014. **44**: 1582–1592.

10 **Hartmann, G. and Krieg, A. M.**, Mechanism and function of a newly identified CpG DNA motif in human primary B cells. *J. Immunol.* 2000. **164**: 944–953.

11 **Wagner, H.**, The immunobiology of the TLR9 subfamily. *Trends Immunol.* 2004. **25**: 1–6.

12 **Krieg, A. M.**, Therapeutic potential of Toll-like receptor 9 activation. *Nat. Rev. Drug Discov.* 2006. **5**: 471–484.

13 **Klinman, D. M.**, Immunotherapeutic uses of CpG oligodeoxynucleotides. *Nat. Rev. Immunol.* 2004. **4**: 1–10.

14 **Desmet, C. J. and Ishii, K. J.**, Nucleic acid sensing at the interface between innate and adaptive immunity in vaccination. *Nat. Rev. Immunol.* 2012. **12**: 479–491.

15 **Barber, G. N.**, Cytoplasmic DNA innate immune pathways. *Immunol. Rev.* 2011. **243**: 99–108.

16 **Sun, L., Wu, J., Du, F., Chen, X. and Chen, Z. J.**, Cyclic GMP-AMP synthase is a cytosolic DNA sensor that activates the type I interferon pathway. *Science* 2013. **339**: 786–791.

17 **Wu, J., Sun, L., Chen, X., Du, F., Shi, H., Chen, C. and Chen, Z. J.**, Cyclic GMP-AMP is an endogenous second messenger in innate immune signaling by cytosolic DNA. *Science* 2013. **339**: 826–830.

18 **Zhang, X., Shi, H., Wu, J., Zhang, X., Sun, L., Chen, C. and Chen, Z. J.**, Cyclic GMP-AMP containing mixed phosphodiester linkages is an endogenous high-affinity ligand for STING. *Mol. Cell.* 2013. **51**: 226–235.

19 **Burdette, D. L., Monroe, K. M., Sotelo-Troha, K., Iwig, J. S., Eckert, B., Hyodo, M., Hayakawa, Y. et al.**, STING is a direct innate immune sensor of cyclic di-GMP. *Nature* 2011. **478**: 515–518.

20 **Mcwhirter, S. M., Barbalat, R., Monroe, K. M., Fontana, M. F., Hyodo, M., Joncker, N. T., Ishii, K. J. et al.**, A host type I interferon response is induced by cytosolic sensing of the bacterial second messenger cyclic-di-GMP. *J. Exp. Med.* 2009. **206**: 1899–1911.

21 **Li, X. D., Wu, J., Gao, D., Wang, H., Sun, L. and Chen, Z. J.**, Pivotal roles of cGAS-cGAMP signaling in antiviral defense and immune adjuvant effects. *Science* 2013. **341**: 1390–1394.

22 **Tang, C. K., Aoshi, T., Jounai, N., Ito, J., Ohata, K., Kobiyama, K., Dessailly, B. H. et al.**, The chemotherapeutic agent DMXAA as a unique IRF3-dependent type-2 vaccine adjuvant. *PLoS One* 2013. **8**: 1–6.

23 **Hogenesch, H.**, Mechanism of immunopotentiation and safety of aluminum adjuvants. *Front. Immunol.* 2013. **3**: 1–13.

24 **Macleod, M. K. L., Mckee, A. S., David, A., Wang, J., Mason R. and Kappler, J. W.**, Vaccine adjuvants aluminum and monophosphoryl lipid A provide distinct signals to generate protective cytotoxic memory CD8 T cells. *Proc. Natl. Acad. Sci. USA* 2011. **108**: 7914–7919.

25 **Weeratna, R. D., Mccluskie, M. J., Xu, Y. and Davis, H. L.**, CpG DNA induces stronger immune responses with less toxicity than other adjuvants. *Vaccine* 2000. **18**: 1755–1762.

26 **Verthelyi, D., Ishii, K. J., Gursel, M., Takeshita, F. and Klinman, D. M.**, Human peripheral blood cells differentially recognize and respond to two distinct CpG Motifs. *J. Immunol.* 2001. **166**: 2372–2377.

27 Hunter, A., Gabriel, K. E., Radzanowski, T., Neyer, L. E. and Remington, J. S., Type I interferons enhance production of IFN-γ by NK cells. *Immunol. Lett.* 1997. 59: 1–5.

28 Nguyen, K. B., Salazar-Mather, T. P., Dalod, M. Y., Van Deusen, J. B., Wei X. Q., Liew, F. Y., Caligiuri, M. A. et al., Coordinated and distinct roles for IFN-, IL-12, and IL-15 regulation of NK cell responses to viral infection. *J. Immunol.* 2002. 169: 4279–4287.

29 Kawai, T., Sato, S., Ishii, K. J., Coban, C., Hemmi, H., Yamamoto, M., Terai, K. et al., Interferon-alpha induction through Toll-like receptors involves a direct interaction of IRF7 with MyD88 and TRAF6. *Nat. Immunol.* 2004. 5: 1061–1068.

30 Chen, S., Kawashima, H., Lowe, J. B., Lanier, L. L. and Fukuda, M., Suppression of tumor formation in lymph nodes by L-selectin—mediated natural killer cell recruitment. *J. Exp. Med.* 2005. 202: 1679–1689.

31 Dubensky, T. W., Kanne, D. B. and Leong, M. L., Advances in vaccines rationale, progress and development of vaccines utilizing STING-activating cyclic dinucleotide adjuvants. *Ther. Adv. Vaccines.* 2013. 1: 131–143.

32 Way, S. S., Havenar-Daughton, C., Kolumam, G. A., Orgun, N. N. and Murali-Krishna, K., IL-12 and Type-I IFN synergize for IFN- production by CD4 T cells, whereas neither are required for IFN- production by CD8 T cells after Listeria monocytogenes infection. *J. Immunol.* 2007. 178: 4498–4505.

33 Krummen, M., Balkow, S., Shen, L., Heinz, S., Loquai, C., Probst, H.-C. and Grabbe, S., Release of IL-12 by dendritic cells activated by TLR ligation is dependent on MyD88 signaling, whereas TRIF signaling is indispensable for TLR synergy. *J. Leukoc. Biol.* 2010. 88: 189–199.

34 Hornung, V., Rothenfusser, S., Britsch, S., Krug, A., Jahrsdorfer, B., Giese, T., Endres, S. et al., Quantitative expression of Toll-like receptor 1–10 mRNA in cellular subsets of human peripheral blood mononuclear cells and sensitivity to CpG oligodeoxynucleotides. *J. Immunol.* 2002. 168: 4531–4537.

35 Chace, J. H., Hooker, N. A., Mildenstein, K. L., Krieg, A. M. and Cowdery, J. S., Bacterial DNA-induced NK cell IFN-g production is dependent on macrophage secretion of IL-12. *Clin. Immunol. Immunopathol.* 1997. 84: 185–193.

36 Swanson, C. L., Wilson, T. J., Strauch, P., Colonna, M., Pelanda, R. and Torres, R. M., Type I IFN enhances follicular B cell contribution to the T cell-independent antibody response. *J. Exp. Med.* 2010. 207: 1485–1500.

37 Chu, B. R. S., Targoni, O. S., Krieg, A. M., Lehmann, P. V. and Harding, C. V., CpG oligodeoxynucleotides act as adjuvants that switch on T helper 1 (Th1) immunity. *J. Exp. Med.* 1997. 186: 1623–1631.

38 Muller, K. M., Jaunin, F., Masouyc, I., Saurat, J. and Hauser, C., Cells mediate IL-4-dependent local tissue inflammation. *J. Immunol.* 1993. 150: 5576–5584.

39 Seki, Y., Inoue, H., Nagata, N., Hayashi, K., Fukuyama, S., Komine, O., Hamano, S. et al., SOCS-3 regulates onset and maintenance of Th2- mediated allergic responses. *Nat. Med.* 2003 9: 1047–1054.

40 Lin, L., Gerth, A. J. and Peng, S. L., CpG DNA redirects class-switching towards "Th1-like" Ig isotype production via TLR9 and MyD88. *Eur. J. Immunol.* 2004. 34: 1483–1487.

41 Gracie J. A. and Bradley J. A., Interleukin-12 induces interferon-γ-dependent switching of IgG alloantibody subclass. *Eur. J. Immunol.* 1996. 26: 1217–1221.

42 Van de Wetering, D., de Paus, R. A., van Dissel, J. T. and van de Vosse, E., IL-23 modulates CD56+/CD3- NK cell and CD56+/CD3 +NK-like T cell function differentially from IL-12. *Int. Immunol.* 2009. 21: 145–153.

43 Lankford, C. S. R. and Frucht, D. M., A unique role for IL-23 in promoting cellular immunity. *J. Leukoc. Biol.* 2003. 73: 49–56.

44 Cho, H. J., Takabayashi, K., Cheng, P., Nguyen, M., Corr, M, Tuck, S and Raz, E., Immunostimulatory DNA-based vaccines induce cytotoxic lymphocyte activity by a T-helper cell-independent mechanism. *Nat. Biotechnol.* 2000. 18: 509–514.

45 De Titta, A., Ballester, M., Julier, Z., Nembrini, C., Jeanbart, L., van der Vlies, A. J., Swartz, M. A. et al., Nanoparticle conjugation of CpG enhances adjuvancy for cellular immunity and memory recall at low dose. *Proc. Natl. Acad. Sci. USA* 2013. 110: 19902–19907.

46 Sauer, J. D., Sotelo-Troha, K., von Moltke, J., Monroe, K. M., Rae, C. S., Brubaker, S. W., Hyodo, M. et al., The N-ethyl-N-nitrosourea-induced Goldenticket mouse mutant reveals an essential function of Sting in the in vivo interferon response to Listeria monocytogenes and cyclic dinucleotides. *Infect. Immun.* 2011. 79: 688–694.

47 Honda, K., Yanai, H., Negishi, H., Asagiri, M., Sato, M., Mizutani, T., Shimada, N. et al., IRF-7 is the master regulator of type-I interferon-dependent immune responses. *Nature.* 2005. 434: 772–777.

48 Kobiyama, K., Aoshi, T., Narita, H., Kuroda, E., Hayashi, M., Tetsutani, K., Koyama, S. et al., Nonagonistic dectin-1 ligand transforms CpG into a multitask nanoparticulate TLR9 agonist. *Proc. Natl. Acad. Sci. USA* 2014. 111:3086–3091.

49 Kuroda, E., Ishii, K. J., Uematsu, S., Ohata, K., Coban, C., Akira, S., Aritake, K. et al., Article silica crystals and aluminum salts regulate the production of prostaglandin in macrophages. *Immunity* 2011. 34: 514–526.

*Abbreviations:* **cGAMP**: cyclic GMP—AMP · **FL-DC**: Flt3L-derived DC · **GM-DC**: GM-CSF-derived dendritic cell · **IFNAR**: IFNα/β receptor · **pDC**: plasmacytoid DC · **STING**: Stimulator of IFN genes

*Full correspondence:* Prof. Ken J. Ishii, Laboratory of Vaccine Science, WPI Immunology Frontier Research Center (iFReC), Osaka University, Osaka 565-0871, Japan
Fax: +81-6-6879-4812
e-mail: kenishii@biken.osaka-u.ac.jp

Received: 14/8/2014
Revised: 3/11/2014
Accepted: 17/12/2014
Accepted article online: 22/12/2014

⌘ *Author's Choice*

THE JOURNAL OF BIOLOGICAL CHEMISTRY VOL. 290, NO. 12, pp. 7463–7473, March 20, 2015


# RNA Polymerase III Regulates Cytosolic RNA:DNA Hybrids and Intracellular MicroRNA Expression*

Received for publication, January 3, 2015, and in revised form, January 23, 2015 Published, JBC Papers in Press, January 26, 2015, DOI 10.1074/jbc.M115.636365

**Christine Xing'er Koo[‡§¶], Kouji Kobiyama[¶‖], Yu J. Shen[‡§], Nina LeBert[‡], Shandar Ahmad[**], Muznah Khatoo[‡], Taiki Aoshi[¶‖], Stephan Gasser[‡§1], and Ken J. Ishii[¶‖2]**

*From the [‡]Immunology Programme and Department of Microbiology, Centre for Life Sciences, and the [§]NUS Graduate School for Integrative Sciences and Engineering, National University of Singapore, Singapore 117456, the [¶]Laboratory of Adjuvant Innovation and the [**]Laboratory of Bioinformatics, National Institute of Biomedical Innovation (NIBIO), Ibaraki, Osaka 567-0085, Japan, and the [‖]Laboratory of Vaccine Science, World Premier International Immunology Frontier Research Center (iFREC), Osaka University, Suita, Osaka 565-0871, Japan*

**Background:** RNA:DNA hybrids exist in the nucleus and mitochondria but not in the cytosol, except in viral infection.
**Results:** RNA:DNA hybrids exist in the cytosol of various human cells and are mediated by RNA polymerase III (Pol III), which regulates the microRNA machinery.
**Conclusion:** Cytosolic RNA:DNA hybrids are regulated by Pol III.
**Significance:** Previous unknown cytosolic RNA:DNA hybrids may have physiological relevance to miRNA machinery and RNA transport.

**RNA:DNA hybrids form in the nuclei and mitochondria of cells as transcription-induced R-loops or G-quadruplexes, but exist only in the cytosol of virus-infected cells. Little is known about the existence of RNA:DNA hybrids in the cytosol of virus-free cells, in particular cancer or transformed cells. Here, we show that cytosolic RNA:DNA hybrids are present in various human cell lines, including transformed cells. Inhibition of RNA polymerase III (Pol III), but not DNA polymerase, abrogated cytosolic RNA:DNA hybrids. Cytosolic RNA:DNA hybrids bind to several components of the microRNA (miRNA) machinery-related proteins, including AGO2 and DDX17. Furthermore, we identified miRNAs that are specifically regulated by Pol III, providing a potential link between RNA:DNA hybrids and the miRNA machinery. One of the target genes, exportin-1, is shown to regulate cytosolic RNA:DNA hybrids. Taken together, we reveal previously unknown mechanism by which Pol III regulates the presence of cytosolic RNA:DNA hybrids and miRNA biogenesis in various human cells.**

RNA:DNA hybrids can occur during transcription and replication of DNA (1). The DNA primase generates short RNA:DNA fragments during replication of the lagging strand (2, 3). Short hybrids also form during the transcription of DNA by RNA polymerases. In contrast, long RNA:DNA hybrids can occur during stalling of the RNA polymerase or during replication of mitochondria DNA (1). Stalling of the RNA polymerases can lead to the formation of R-loops, which consist of long RNA:DNA hybrids and the displaced non-template DNA strand. Long RNA:DNA hybrids also occur in G-quadruplexes, which promote class switch recombination in B-cells (5). Recent evidence suggests that R-loops and G-quadruplexes may occur more frequently than previously assumed and interfere with gene expression and threaten genome stability (6–8). Although many studies have focused on the generation of nuclear RNA:DNA hybrids, it is unclear how nuclear RNA:DNA hybrids are resolved, and their role in diseases related to genomic instability, such as cancer, is not understood.

We recently discovered the presence of ssDNA and dsDNA in the cytosol of B-cell lymphoma cells (9). Inhibition of ATM (ataxia telangiectasia-mutated) and ATR (ataxia telangiectasia- and Rad3-related) kinases, which initiate the DNA damage response (DDR),[3] leads to the disappearance of cytosolic DNA. Conversely, the levels of cytosolic ssDNA and dsDNA increase in response to DNA damage, suggesting that constitutive nuclear DNA damage and the ensuing DDR induce the presence of cytosolic ssDNA and dsDNA in B-cell lymphoma cells. Cytosolic DNA in B-cell lymphoma cells activates STING-dependent DNA sensor pathways, leading to the expression of ligands for the activating immune receptor NKG2D (natural killer group 2, member D) (9). Delocalized DNA is important for innate immune recognition of pathogens, and recent reports suggest that TLR9 and the NLRP3 inflammasome sense pathogen-derived RNA:DNA hybrids in dendritic cells (10–13). However, whether RNA:DNA hybrids exist in the cytosol of non-infected cells is unknown.

RNA polymerase III (Pol III) is the largest RNA polymerase, consisting of 17 subunits, including a DNA-binding site (14–16). It catalyzes the transcription of genes required for transcription and RNA processing, such as tRNAs, ribosomal 5 S

* This work was supported by the Health and Labour Sciences Research Grant Adjuvant Database Project from the Japanese Ministry of Health, Labour and Welfare and by the National Research Foundation Grant HUJ-CREATE-Cellular and Molecular Mechanisms of Inflammation (to S. G.).
⌘ *Author's Choice*—Final version full access.
[1] To whom correspondence may be addressed. E-mail: stephan_gasser@nuhs.edu.sg.
[2] To whom correspondence may be addressed. E-mail: kenishii@biken.osaka-u.ac.jp.

[3] The abbreviations used are: DDR, DNA damage response; Pol III, RNA polymerase III; miRNA/miR, microRNA; DMSO, dimethyl sulfoxide; COX IV, cytochrome *c* oxidase; Bis-Tris, 2-[bis(2-hydroxyethyl)amino]-2-(hydroxymethyl)propane-1,3-diol.

rRNA, and U6 snRNAs. It also transcribes short interspersed elements and repeated elements in the human genome (14). Pol III expression is regulated by oncogene products, tumor suppressors such as p53, and Pol III-associated transcription factors (17–19). Consistent with these observations, Pol III activity is increased in many cancers, including melanomas, myelomas, and carcinomas (20). Although Pol III is present mostly in the nucleus (20, 21), cytosolic Pol III was proposed to play a role in the sensing of AT-rich DNA via the RIG-I (retinoic acid-inducible gene I) pathway (22–24). Despite the regulation of Pol III by genes associated with tumorigenesis, little is known about the role of Pol III in the cellular function of transformed cells.

Here, we identified the presence of cytosolic RNA:DNA hybrids in immortalized and transformed human tumor cells. Chemical inhibition of Pol III abrogated the presence of cytosolic RNA:DNA hybrids in cells. Cytosolic RNA:DNA hybrids were bound by microRNA (miRNA) machinery-associated proteins, such as DDX17 (DEAD (Asp-Glu-Ala-Asp) box polypeptide 17) and AGO2 (argonaute 2). We also identified Pol III-regulated intracellular miRNAs in A549 lung cancer cells. In summary, we demonstrate the constitutive presence of cytosolic RNA:DNA hybrids in a variety of cell lines, and this accumulation depends on Pol III, at least in A549 lung carcinoma cells.

## EXPERIMENTAL PROCEDURES

*Cells*—The human lung adenocarcinoma (A549), colorectal adenocarcinoma (LoVo and HT29), colorectal carcinoma (HCT116), acute monocytic leukemia (THP-1), human cervix carcinoma (HeLa), and normal lung tissue-derived (MRC-5) cell lines were purchased from American Type Culture Collection (Manassas, VA). Cells were grown in Dulbecco's modified Eagle's medium (Nacalai Tesque) supplemented with 10% fetal bovine serum (Nichirei Biosciences Inc., Tokyo, Japan), 1% penicillin/streptomycin (Nacalai Tesque), and 2% HEPES (Life Technologies). Cells were maintained with 5 μg/ml Plasmocin (InvivoGen) to prevent mycoplasma infection.

*Reagents and Cell Treatments*—Ara-C (cytarabine) was purchased from Wako Chemicals. Aphidicolin, Pol III inhibitor ML-60218, and leptomycin B were purchased from Calbiochem. ATM inhibitor KU60019 (Tocris Bioscience) and ATR inhibitor VE821 (Axon Medchem) were used at 10 μM. PicoGreen dsDNA reagent (Life Technologies) was used at 1:100 dilution. MitoTracker Red CM-H2XRos (Life Technologies) was dissolved in dimethyl sulfoxide (DMSO) and used at 500 nM. Fixed cells were treated with 0.5 units/ml RNase H (New England Biolabs) for 3 h at 37 °C.

*Immunofluorescence Studies*—Cells were fixed in 4% paraformaldehyde (Nacalai Tesque) for 10 min and permeabilized in 0.2% Triton X-100 for 15 min. Nonspecific sites were blocked with 2% goat serum and 1% BSA in 0.2% Triton X-100 for 1 h. Transfected cells were stained with anti-cytochrome *c* oxidase subunit IV (COX IV) antibody (ab16056, Abcam), anti-POLR3G antibody (polymerase (RNA) III (3) (DNA-directed) polypeptide G; LS-C163858, LSBio), or anti-DDX17 antibody (19910-1-AP, Proteintech). The RNA:DNA hybrid-specific antibody S9.6 was a kind gift of Dr. D. Koshland (University of California, Berkeley) (25). The secondary polyclonal antibodies used were Alexa Fluor 488-conjugated goat anti-mouse IgG $F(ab')_2$ fragment (H+L) and Alexa Fluor 555-conjugated goat anti-rabbit IgG $F(ab')_2$ fragment (H+L) (Life Technologies). PicoGreen staining of DNA and MitoTracker staining of mitochondria were performed according to the manufacturer's instructions. Cells were stained with 2 μg/ml Hoechst for 10 min and mounted in mounting medium (Dako). Cell images were taken with a Leica TCS SP2 laser confocal scanning microscope and analyzed using Volocity (version 6.2.1) and Imaris. Micrographs show cells representative of total cell populations.

*Transfection*—A549 cells were transfected with POLR3G siRNA (Qiagen) using Lipofectamine RNAiMAX transfection reagent (Life Technologies) according to the manufacturer's instructions. AllStars negative control siRNA (Qiagen) was used as a control in transfection, and its sequence is proprietary. The POLR3G siRNA sequences used were 5′-AAGGCACACCACTCACTAATA-3′ (siPOLR3G_1) and 5′-TCAGAGTACTCAAGTGTACAA-3′ (siPOLR3G_2).

*Immunoblotting*—Cells were lysed in cold radioimmune precipitation assay buffer (Nacalai Tesque), and lysates were electrophoresed in 4–12% NuPAGE Bis-Tris gel (Life Technologies) and then blotted onto PVDF membranes. Antibodies specific to DDX17 (sc-86409, Santa Cruz), AGO2 (C34C6, Cell Signaling Technology), and GAPDH (M171-3, MBL International) and horseradish peroxidase-conjugated secondary antibodies (Cell Signaling Technology) were used to develop the blots with Immobilon Western chemiluminescent HRP substrate (Millipore). Digital images were acquired using ImageQuant LAS 500 (GE Healthcare).

*Immunoprecipitation and Mass Spectrometry*—A549 cells ($2 \times 10^6$) were seeded into 100-mm dishes and fixed in 1% paraformaldehyde for 10 min, followed by treatment with 125 mM glycine (Wako Chemicals) for 5 min. Cells were fractionated using a cell fractionation kit (MS861, MitoSciences). The cytosolic fraction was precleared by incubation with 5 μl of protein G-Sepharose beads (GE Healthcare) for 20 min at 4 °C on a rolling shaker. The cleared supernatant was incubated overnight at 4 °C on a rolling shaker with 10 μg/ml RNA:DNA hybrid-specific antibody and 10 μl of protein G-Sepharose beads. Immunoprecipitates were washed sequentially with radioimmune precipitation assay buffer, low salt buffer (20 mM Tris-HCl (pH 8.1), 150 mM NaCl, 0.1% SDS, 1% Triton X-100, and 2 mM EDTA), high salt buffer (20 mM Tris-HCl (pH 8.1), 600 mM NaCl, 0.1% SDS, 1% Triton X-100, and 2 mM EDTA), final wash buffer (20 mM Tris-HCl (pH 8.0), 0.1% SDS, 1% Triton X-100, and 1 mM EDTA), and Tris/EDTA buffer. Beads were resuspended in Tris/EDTA buffer with 1% SDS and incubated overnight at 65 °C to release protein complexes for subsequent gel electrophoresis. For mass spectrometry, similarly processed cell lysates were immunoprecipitated with RNA:DNA hybrid-specific antibody and silver-stained using a Silver Stain Plus kit (Bio-Rad) according to the manufacturer's instructions. Bands of interest were cut out and sent for mass spectrometry analysis at the Osaka University mass spectrometry facility.

*miRNA Microarray Analysis*—A549 cells were treated with 10 μM Pol III inhibitor for 24 h and subsequently treated with 10 μM Ara-C or DMSO for 15 h. DMSO-treated cells served as a control. Total RNA was extracted with TRIzol (Life Technologies) and labeled using a 3D-Gene miRNA labeling kit. The

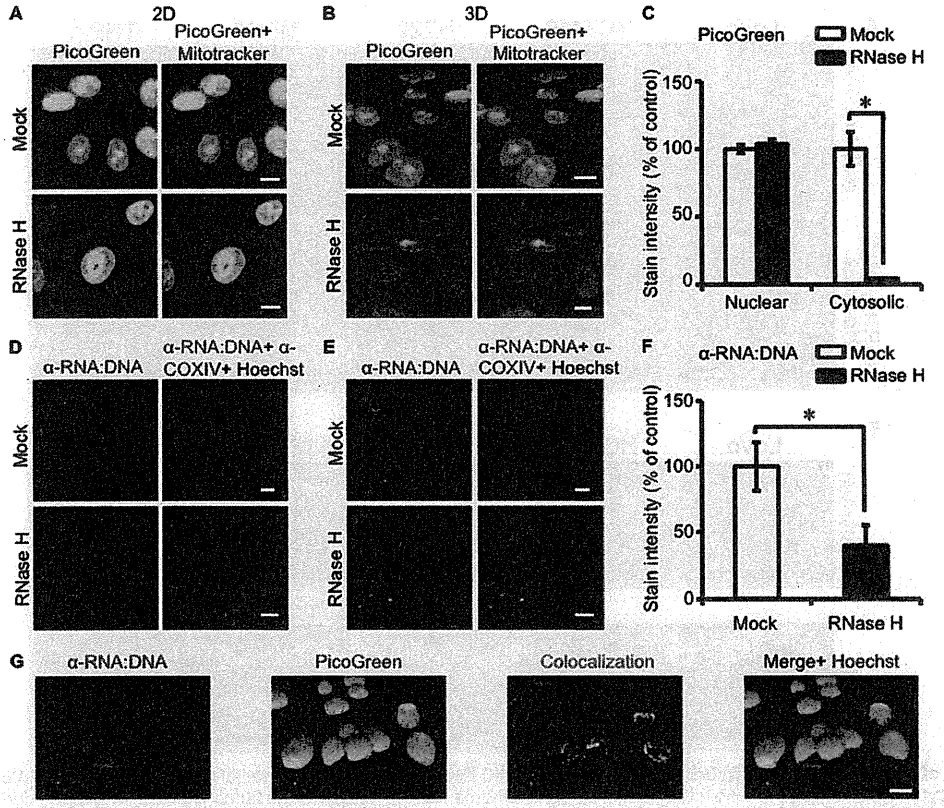


FIGURE 1. **RNA:DNA hybrids exist in the cytosol of human lung cancer cells.** *A*, the human lung carcinoma cell line A549 was stained with the vital dsDNA-specific dye PicoGreen (*green*) at 10 μl/ml for 1 h and with the mitochondria-specific vital dye MitoTracker (*red*) at 100 nM for 30 min. Samples shown in the *lower panels* were pretreated with 0.5 units/ml RNase H. *Scale bars* = 10 μm. *B* and *C*, three-dimensional isosurface rendering (*B*) and quantification (*C*) of PicoGreen staining in the nucleus and cytosol of the images shown in *A*. A one-tailed Wilcoxon test was performed. *Error bars* represent S.E. *, $p < 0.05$. *D*, A549 cells were stained with the RNA:DNA hybrid-specific antibody S9.6 (*green*) and the mitochondrial marker COX IV (*red*) in the presence of Hoechst (*blue*). Cells shown in the *lower panels* were pretreated with 0.5 units/ml RNase H before staining. *E* and *F*, three-dimensional isosurface rendering (*E*) and quantification (*F*) of RNA:DNA hybrid staining of the images shown in *D*. *G*, three-dimensional isosurface rendering of staining of A549 cells with PicoGreen (*green*), RNA:DNA hybrid-specific antibodies (*red*), and Hoechst (*blue*). A one-tailed Wilcoxon test was performed.

labeled RNA was hybridized to a human miRNA V19 microarray chip containing 2019 miRNA probes and analyzed on a ProScanArray microarray scanner (Toray Industries). miRNA profiles were provided as sample-wise median-normalized data by Toray Industries. Data were further normalized with an all-sample quantile normalization protocol using the corresponding Bioconductor package developed by Bolstad *et al.* (26). Original miRNA profiles consisted of 2019 miRNA probes, of which only a small fraction showed significant expression in any of these experiments. After replacing the missing valued data (no expression observed) with the minimum of all observed expression values, miRNA probes that showed at least 3-fold differential expression between any pair of four experiments were used for further quantitative analysis. Identified miRNA sequences were used to obtain predicted gene targets, as acquired from the public domain resource DIANA-mirPath (27). A $p$ value threshold of 0.05 and a MicroT threshold of 0.8 were applied.

*miRNA Expression Analysis*—After RNA extraction, cDNA was synthesized using a miScript II RT kit (Qiagen). miRNA levels were analyzed using assay kits for mature miR-4499 (Qiagen), precursor (includes detection for precursor and primary miR) miR-4499 (Qiagen), and TaqMan primary miR-4499 (Life Technologies) and quantified by quantitative PCR using iTaq Universal SYBR Green Supermix (Bio-Rad) or TaqMan Gene Expression Master Mix (Life Technologies). Precursor miR expression was determined using the equation in Ref. 28.

*Quantitative Real-time RT-PCR*—Experiments were performed as described previously (9). The following primers were used: *XPO1*-5′ (exportin-1), 5′-AGGTTGGAGAAGTGATGCCA-3′; *XPO1*-3′, 5′-GCACCAATCATGTACCCCAC-3′; *KPNB1*-5′ (karyopherin (importin) beta 1), 5′-GACCGACTACCCAGACAGAG-3′; *KPNB1*-3′, 5′-GACTCCTCCTAAGACGACGG-3′; *NUP153*-5′ (nucleoporin 153kDa), 5′-GCCCAAATCTTCCTCTGCAG-3′; *NUP153*-3′, 5′-GAAAGGAGCCACTGAAGCAC-3′; *HPRT1*-5′, 5′-CCCTGGCGTCGTGATTAGTG-3′; and *HPRT1*-3′, 5′-TCGAGCAAGACGTTCAGTCC-3′.

*Statistical Analysis*—For statistical analysis, Student's one-tailed $t$ test ($p < 0.05$) was used unless stated otherwise after data were tested positive for normality by the Shapiro-Wilk test. For data that failed the normality test, a non-parametric Mann-Whitney Wilcoxon rank-sum test was used. A $p$ value of $<0.05$ was considered statistically significant.

## RESULTS

*Presence of RNA:DNA Hybrids in the Cytosol of Human Cells*—We previously reported (9) the presence of cytosolic ssDNA and dsDNA in cancer cells using specific antibodies and the vital dye PicoGreen, which detects dsDNA and RNA:DNA

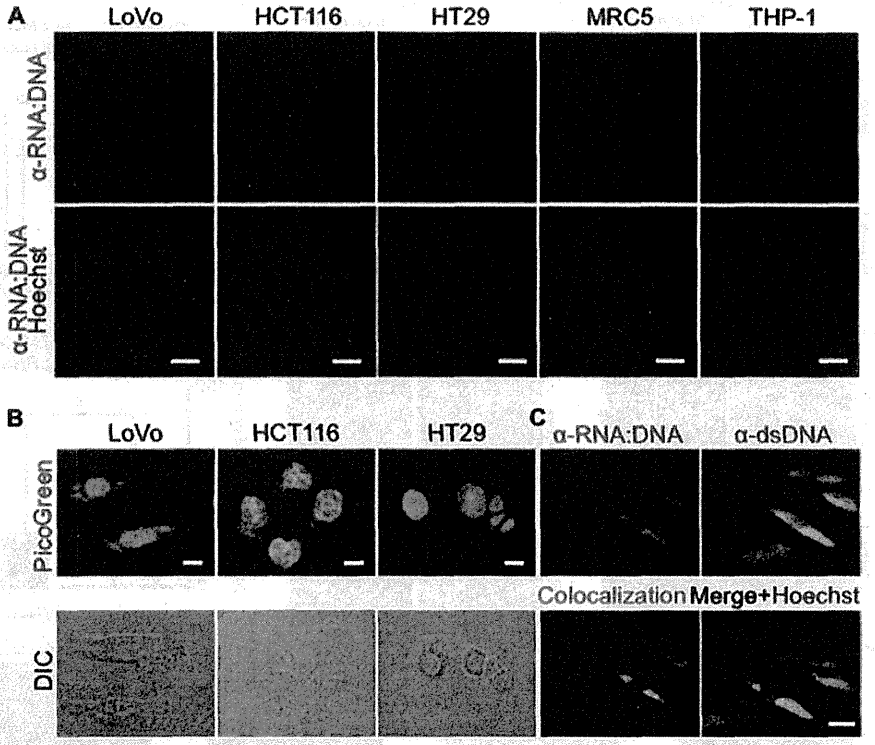


FIGURE 2. **Presence of cytosolic RNA:DNA hybrids in human tumor cell lines.** *A*, the human colorectal carcinoma cell lines LoVo, HCT116, and HT29; the human acute monocytic leukemia cell line THP-1; the human cervix carcinoma cell line HeLa; and the human normal lung tissue-derived cell line MRC-5 were stained for RNA:DNA hybrids (*red*) in the presence of Hoechst (*blue*). *Scale bars* = 10 μm. *B*, the colorectal adenocarcinoma cell lines LoVo, HCT116, and HT29 were stained with PicoGreen (*upper panels*). Bright-field images (differential interference contrast (*DIC*)) of cells are shown in the *lower panels*. *C*, three-dimensional isosurface rendering of confocal images of A549 cells stained for the presence of dsDNA (*green*) and RNA:DNA hybrids (*red*) in the presence of Hoechst (*blue*). Co-localization of dsDNA and RNA:DNA hybrids (*yellow*) was determined using Volocity computational image analysis.

hybrids (29, 30). Here, we sought to test if RNA:DNA hybrids are present in the cytosol of human cancer cell lines. PicoGreen stained DNA in the cytosol of the human lung carcinoma cell line A549 and other cancer cell lines (Fig. 1, *A* and *B*, and Fig. 2, *A* and *B*). Three-dimensional surface rendering of confocal images showed that the majority of extranuclear DNA is present outside of mitochondria (Fig. 1*B*). To analyze if RNA:DNA hybrids contribute to the PicoGreen signals in the cytosol, A549 cells were treated with RNase H, which degrades RNA in RNA:DNA hybrids (31), prior to staining with PicoGreen. Pretreatment of cells with RNase H abrogated the cytosolic PicoGreen signals (Fig. 1, *A–C*). As expected, the staining of nuclear genomic DNA by PicoGreen was not changed.

To further investigate the presence of cytosolic RNA:DNA hybrids, we stained cells using the RNA:DNA hybrid-specific antibody S9.6 (25). In agreement with the PicoGreen results, S9.6 staining of tumor cells (A549, LoVo, HCT116, HT29, HeLa, and THP-1) and human fetal lung fibroblast cells (MRC-5) showed the presence of RNA:DNA hybrids in the cytosol and, to a lesser extent, in the nucleus (Fig. 1, *D* and *E*, and Fig. 2, *A* and *B*). As RNA:DNA hybrids can also form during replication of mitochondrial DNA (32), we co-stained cells with the mitochondria-specific vital dye MitoTracker. Three-dimensional surface rendering of confocal images showed that the majority of RNA:DNA hybrids were localized outside of mitochondria (Fig. 1*E*). Pretreatment of cells with RNase H prior to S9.6 staining significantly reduced the cytosolic RNA:DNA hybrid staining (Fig. 1, *D–F*). Antibody S9.6 only partially co-stained with PicoGreen (Fig. 1*G*), suggesting that PicoGreen stains cytosolic dsDNA and RNA:DNA hybrids in A549 cells. Consistent with this possibility, staining of A549 cells using a dsDNA-specific antibody showed the presence of cytosolic dsDNA, which partially co-localized with the cytosolic PicoGreen staining (Fig. 2*C*). In summary, our data show that RNA:DNA hybrids are constitutively present in the cytosol of all tested cells.

*Presence of Cytosolic RNA:DNA Hybrids Depends on Pol III*—RNA:DNA hybrids can occur during DNA transcription (33). In addition, cytosolic DNA is transcribed by Pol III in the cytosol and potentially in the nucleus into an RNA:DNA hybrid and dsRNA intermediate (22, 23). To understand the mechanism by which cytosolic RNA:DNA hybrids are generated and regulated, A549 cells were treated with Pol III inhibitors prior to staining with S9.6 or PicoGreen (34). Treatment of A549 cells with the Pol III inhibitor ML-60218 decreased the cytosolic RNA:DNA hybrid staining at doses above the published half-maximal inhibitory concentration ($IC_{50}$), but had no effect on nuclear PicoGreen staining and affected RNA:DNA hybrid staining at doses above $IC_{50}$ (Fig. 3). Treatment of A549 cells with α-amanitin, a Pol II inhibitor, was toxic to cells compared with the Pol III inhibitor ML-60218.

To investigate if the genetic inhibition of Pol III also reduced RNA:DNA hybrid levels, A549 cells were transfected with siRNA against POLR3G (siPOLR3G_1 and siPOLR3G_2), a subunit of the Pol III complex, or negative control siRNA.

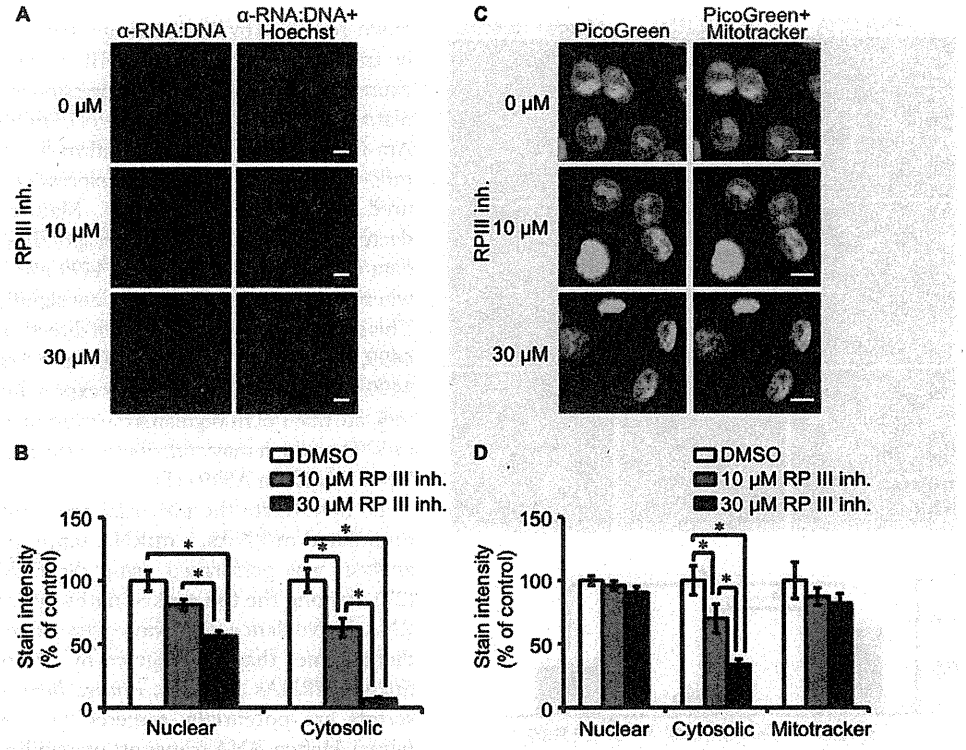


FIGURE 3. **Pol III is essential for the presence of cytosolic RNA:DNA hybrids.** *A*, A549 cells were treated with the indicated concentration of the Pol III inhibitor (*RP III inh.*) ML-60218 for 3 h before staining with 10 μl/ml PicoGreen (*green*) for 1 h and with 100 nM MitoTracker (*red*) for 30 min. *Scale bars* = 10 μm. *B*, cytosolic and nuclear intensity quantification of the images shown in *A*. A two-tailed Wilcoxon test was performed. *Error bars* represent S.E. *, $p < 0.05$. *C*, A549 cells were treated with the indicated concentrations of the Pol III inhibitor ML-60218 for 3 h before staining with RNA:DNA hybrid-specific S9.6 antibody (*green*) and Hoechst (*blue*). *D*, cytosolic and nuclear intensity quantification of the images shown in *C*. A two-tailed Wilcoxon test was performed.

Knockdown of POLR3G protein expression resulted in the disappearance of cytosolic RNA:DNA hybrids by immunofluorescence staining, consistent with reduced *POLR3G* mRNA gene expression (Fig. 4). In contrast, negative control siRNA did not affect cytosolic RNA:DNA hybrid levels or POLR3G expression. This corroborated with previous results of Pol III chemical inhibition, which decreased the presence of RNA:DNA hybrids.

In contrast to Pol II, which is localized exclusively in the nucleus, a fraction of Pol III is present in the cytosol. To investigate if cytosolic Pol III contributes to the generation of RNA:DNA hybrids in the cytosol, we co-stained A549 cells for POLR3G, a subunit of the Pol III complex, and RNA:DNA hybrids (35). No significant co-staining of POLR3G and S9.6 or PicoGreen was observed in the cytosol of A549 cells (Fig. 5*A*). Furthermore, POLR3G was localized largely in the nucleus, suggesting that the presence of cytosolic RNA:DNA hybrids depends on nuclear Pol III activity.

*Presence of Cytosolic RNA:DNA Hybrids Is Independent of DNA Damage*—RNA:DNA hybrids can cause stalling of the replication fork and formation of dsDNA breaks (1, 36, 37). To test if stalling of replication forks and the associated DNA damage contribute to the presence of RNA:DNA hybrids in the cytosol, A549 cells were treated with Ara-C, a genotoxic DNA replication inhibitor used to treat leukemia, and aphidicolin, an inhibitor of DNA polymerases (38). Treatment with Ara-C or aphidicolin had no effect on the level of cytosolic RNA:DNA hybrids in A549 cells (Fig. 5, *A* and *C*). Moreover, Ara-C treatment did not increase the co-localization of POLR3G and RNA:DNA hybrids (Fig. 5, *A* and *B*).

To test if the cellular response to DNA damage is required for the presence of cytosolic RNA:DNA hybrids, we inhibited ATM and ATR, two kinases that initiate the DDR. We previously found that the presence of dsDNA in the cytosol of B-cell lymphoma cells depends on the DDR (9). In contrast, inhibition of the DDR had no effect on the presence of RNA:DNA hybrids in the cytosol (Fig. 5*D*). Hence, unlike cytosolic dsDNA, RNA:DNA hybrid levels in the cytosol depend on Pol III, but not DNA damage or the DDR.

*Cytosolic RNA:DNA Hybrids Bind Members of the miRNA Processing Machinery*—To examine whether RNA:DNA hybrids interact with proteins in the cytosol, we performed immunoprecipitation experiments using the RNA:DNA-specific antibody S9.6 in cytosolic extracts of A549 cells. A fraction of the extracts were treated with RNase H before analysis to verify RNA:DNA hybrid-specific binding of proteins. Analysis by mass spectrometry identified DDX5/DDX17, AGO2, and BRCA1 (breast cancer susceptibility gene 1) as proteins that immunoprecipitated in an S9.6-dependent manner (Fig. 6*A*). All three proteins are part of the miRNA processing machinery (39). Immunoblot analyses of immunoprecipitated proteins showed that DDX17 binding was consistent with the mass spectrometry analysis (Fig. 6*B*). AGO2 is part of the miRNA-mediated DDR (40) and increases interaction with repair molecules during double-strand break repair (41). Ara-C treatment

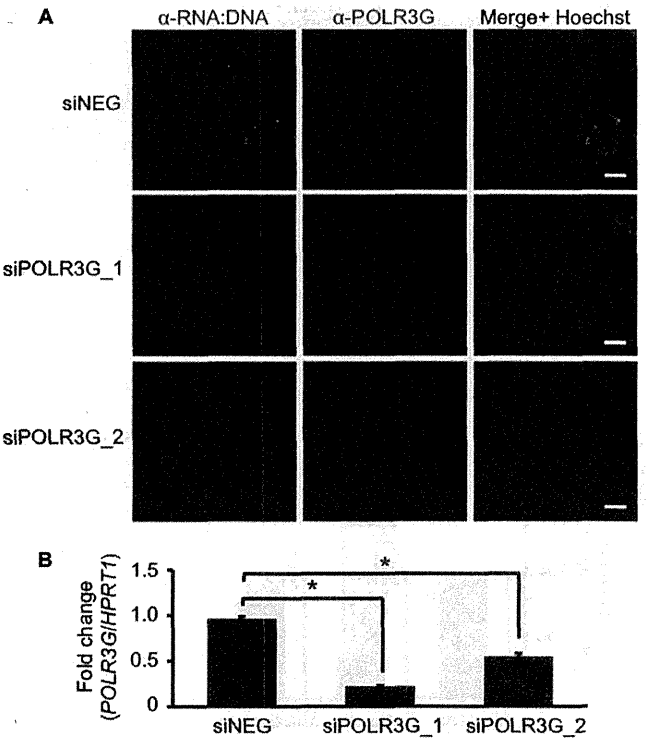


FIGURE 4. **Genetic knockdown of Pol III decreases cytosolic RNA:DNA hybrid levels.** *A*, A549 cells were transfected with 25 nM negative control siRNA (*siNEG*) or siRNA against POLR3G (siPOLR3G_1 and siPOLR3G_2). At 72 h after transfection, cells were stained for RNA:DNA hybrids (*green*) and POLR3G (*red*) in the presence of Hoechst (*blue*). *Scale bars* = 10 μm. *B*, some cells in *A* were subjected to RNA isolation for measurement of *POLR3G* mRNA expression with respect to *HPRT1*. Student's one-tailed *t* test was performed. *Error bars* represent S.E. *, $p < 0.05$.

increased the interaction of S9.6 with AGO2 proteins (Fig. 6*C*). Consequently, components of the miRNA processing machinery were found to interact with cytosolic RNA:DNA hybrids in the absence of DNA damage and increased interaction in the presence of DNA damage.

*Pol III Regulates the Expression of Specific miRNAs*—We next sought to gain insights into the Pol III-dependent mechanisms leading to the presence of cytosolic RNA:DNA hybrids. Our data support the possibility that Pol III-mediated transcription of miRNAs is associated with the presence of cytosolic RNA:DNA hybrids. Pol III is able to transcribe a subset of miRNAs in a cell type-specific manner (42) or interact with canonical genes within a chromosome location that also encodes miRNAs (43). To determine whether a subset of miRNAs are dependent on Pol III, we examined the Pol III-dependent miRNA expression profile in A549 cells by comprehensive miRNA array analysis. To distinguish Pol III effects from RNA:DNA hybrid-induced DNA damage, cells were treated with the genotoxic DNA replication inhibitor Ara-C or the Pol III inhibitor ML-60218. A total of 81 differentially expressed miRNAs were identified after comparison across the treatment groups (Fig. 7*A*). Strikingly, treatment of cells with the Pol III inhibitor resulted in significant down-regulation of only four miRNAs: miR-615-5p, miR-1178-5p, miR-4499, and miR-5571-3p (Fig. 7, *A* and *B*). The expression of miR-615-5p, miR-1178-5p, and miR-5571-3p was also decreased after Ara-C treatment, suggesting that the expression of these miRNAs is also down-regulated by DNA damage. In contrast, miR-4499 is likely to be transcribed directly by Pol III, as Ara-C had no effect on its expression. Surprisingly, the expression of 10 miRNAs was up-regulated after treatment with the Pol III inhibitor ML-60218, but not Ara-C (Fig. 7, *A* and *B*). To confirm that Pol III directly regulates miR-4499 expression, miRNA expression of miR-4499 was measured after Pol III treatment. Mature miR-4499 expression decreased after treatment, corresponding to miRNA microarray data (Fig. 7*C*). Precursor miR-4499 also decreased significantly, whereas primary miR-4499 was not significantly affected (Fig. 7*C*). This suggests that Pol III does not directly transcribe primary miR-4499, but might regulate Drosha processing of precursor miR-4499 to affect mature miR-4499 expression. In summary, our data indicate that Pol III regulates the expression of a limited number of miRNAs, which may contribute to the presence of cytosolic RNA:DNA hybrids in A549 cells.

To investigate the potential transcripts targeted by Pol III-modulated miRNAs, a miRNA target prediction and pathway analysis was performed using the DIANA-mirPath software (27). Among the top ranked pathways, the RNA transport and RNA surveillance pathways were identified to contain predicted genes that are targeted by two or more ML-60218-induced miRNAs (Fig. 8*A*, *orange boxes*), whereas other transcripts are potentially targeted by a single miRNA (*yellow boxes*). Hence, RNA transport or stability may contribute to the presence of RNA:DNA hybrids. To test the predictability of the DIANA-mirPath software, three genes (*KPNB1*, *XPO1*, and *NUP153*) were selected for mRNA expression detection after Pol III inhibition. The gene expression of *XPO1* and *NUP153* was found to be down-regulated by 1.6- and 3.3-fold, respectively (Fig. 8*B*).

*Exportin-1 Regulates Transport of RNA:DNA Hybrids from the Nucleus to the Cytosol*—Of the identified genes that were down-regulated in response to Pol III inhibition, *XPO1* encodes for exportin-1, a protein involved in RNA transport and miRNA processing (44, 45). To test if exportin-1 is involved in transport of nuclear RNA:DNA hybrids to the cytosol, cells were treated with leptomycin B, an XPO1 inhibitor. Increasing concentrations of leptomycin B decreased accumulation of cytosolic RNA:DNA hybrids, whereas cytosolic COX IV remained unchanged (Fig. 9), suggesting that XPO1 function is required for the presence of RNA:DNA hybrids.

## DISCUSSION

Here, we have shown the existence of endogenous RNA:DNA hybrids in the cytosol of a variety of human cells, including cancer cells. We previously found that the presence of ssDNA and dsDNA in the cytosol of B-cell lymphomas depends on DNA damage and the ensuing DDR (9). In contrast, treatment of cells with genotoxic agents or blocking of the DDR had no effect on the levels of cytosolic RNA:DNA hybrids, suggesting that the presence of RNA:DNA hybrids is regulated by different pathways. Consistent with this conclusion, inhibition of Pol III led to the disappearance of RNA:DNA hybrids in the cytosol. Interestingly, Pol III inhibitors also abrogated cytosolic PicoGreen staining, which stained cytosolic dsDNA in A549 cells, suggesting that Pol III contributes to the presence of dsDNA in A549 cells. It is possible that Pol III-de-

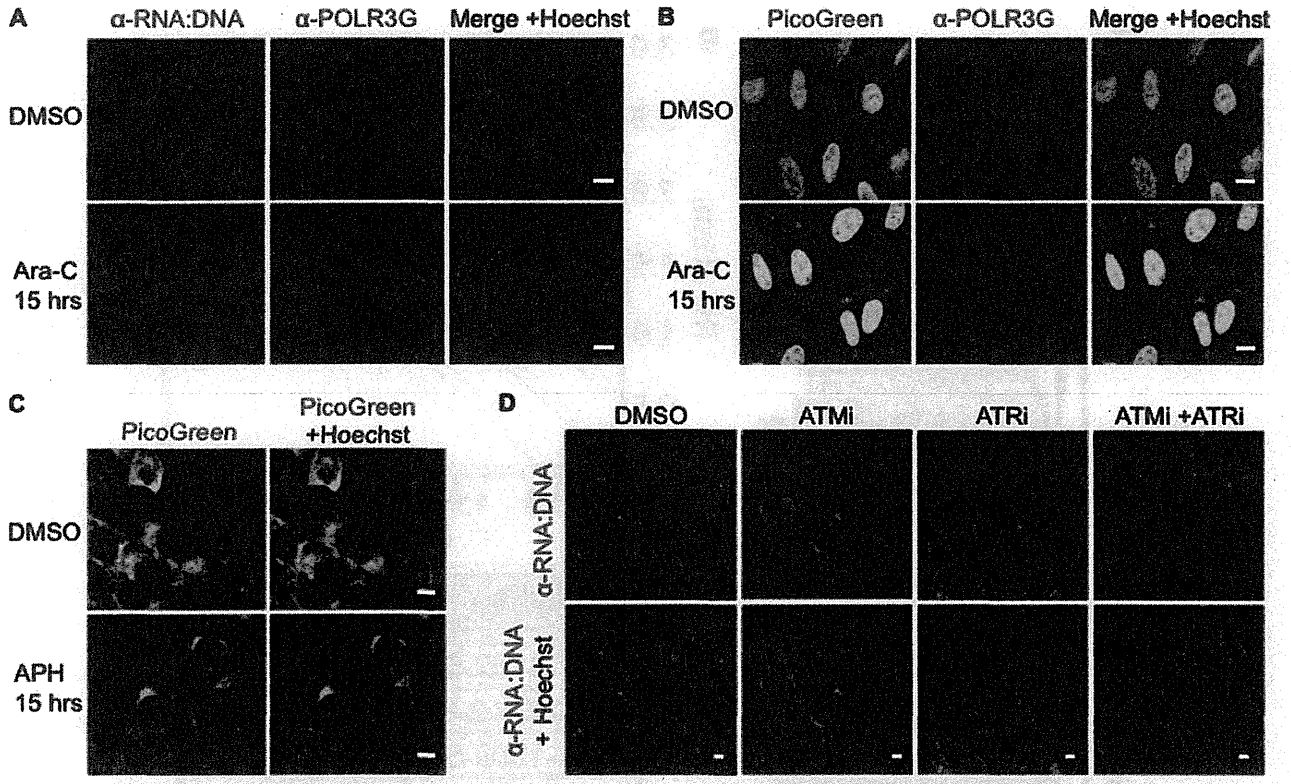


FIGURE 5. **Levels of cytosolic RNA:DNA hybrids are not modulated by genotoxic replication inhibitors.** *A*, A549 cells were treated with the genotoxic DNA replication inhibitor Ara-C at 10 $\mu$M for 15 h and stained for RNA:DNA hybrids (*green*) and POLR3G (*red*) in the presence of Hoechst (*blue*). *Scale bars* = 10 $\mu$m. *B*, A549 cells were treated with Ara-C as in *A* and stained with 10 $\mu$l/ml PicoGreen (*green*), POLR3G-specific antibody (*red*), and Hoechst (*blue*). *C*, A549 cells were treated with 4 $\mu$M aphidicolin (*APH*), an inhibitor of DNA polymerases, for 15 h and stained for RNA:DNA hybrids (*green*) in the presence of Hoechst (*blue*). *D*, A549 cells were treated with 10 $\mu$M ATM inhibitor (*ATMi*), ATR inhibitor (*ATRi*), or both for 15 h. Cells were stained for RNA:DNA hybrids (*red*) in the presence of Hoechst (*blue*).

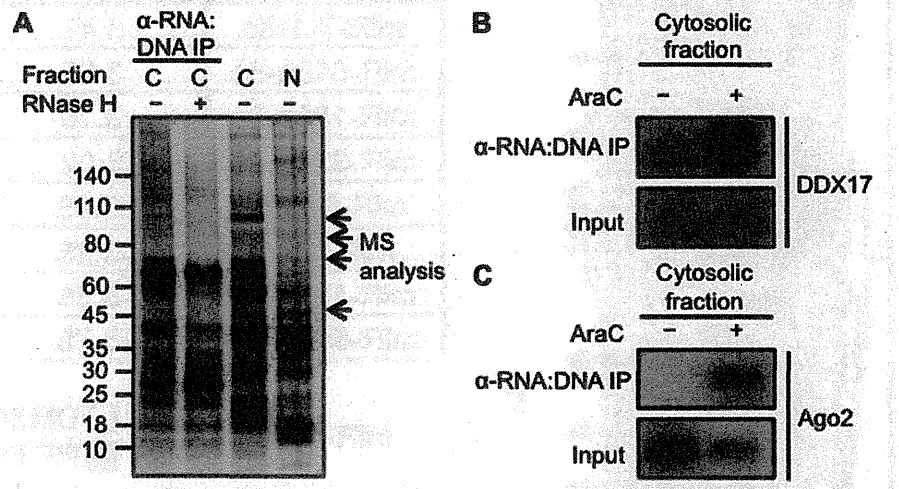


FIGURE 6. **Cytosolic RNA:DNA hybrids interact with miRNA machinery proteins.** *A*, cytosolic fractions of A549 cells were subjected to immunoprecipitation (*IP*) using RNA:DNA hybrid-specific antibody S9.6. Part of the cytosolic fraction was pretreated with 0.5 units/ml RNase H. Immunoprecipitated proteins were detected by SDS-PAGE and silver staining. The indicated bands were analyzed by mass spectrometry. *C*, cytosolic; *N*, nuclear. *B* and *C*, A549 cells were treated with DMSO or 10 $\mu$M Ara-C for 15 h and harvested for cell fractionation after fixation. Cytosolic fractions were subjected to immunoprecipitation with RNA:DNA hybrid-specific antibody S9.6. Immunoblot analysis was carried out on immunoprecipitated proteins probed with antibodies specific for DDX17 (*B*) and AGO2 (*C*).

pendent R-loops, which contain RNA:DNA hybrids, contribute to the presence of cytosolic dsDNA in tumor cells by stalling replication forks, resulting in DNA damage and activation of the DDR (37). In agreement with this possibility, it was recently shown that the DDR is activated in cells that are deficient in the R-loop-resolving enzyme RNase H2 (46). Furthermore, overexpression of *Rnaseh1*, which degrades the RNA strand in RNA:DNA hybrids, decreases the levels of cytosolic ssDNA and dsDNA in tumor cells.[4]

[4] Y. J. Shen, N. Le Bert, A. A. Chitre, C. X. Koo, X. H. Nga, S. S. W. Ho, K. J. Ishii, D. H. Raulet, and S. Gasser, submitted for publication.

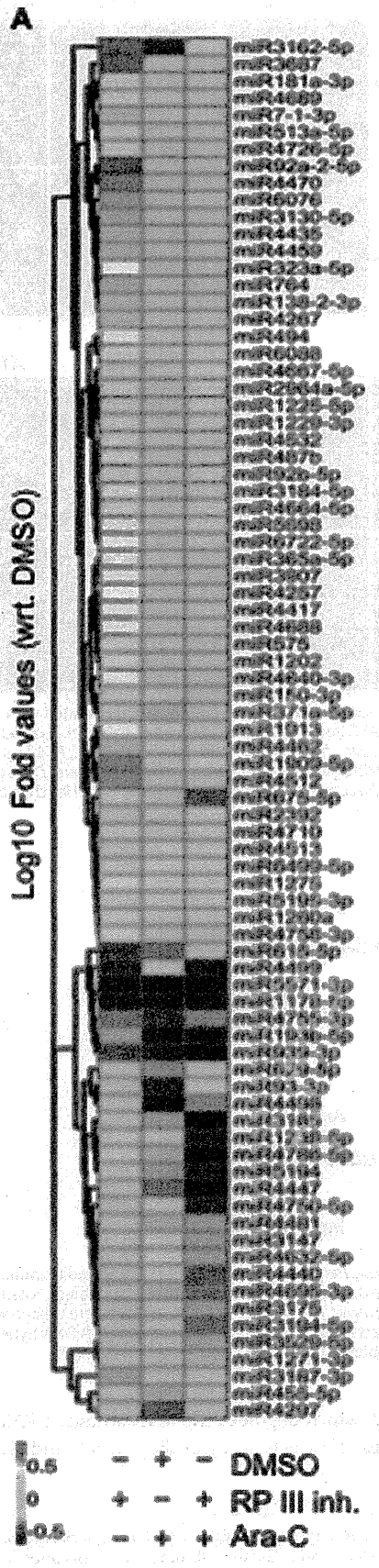


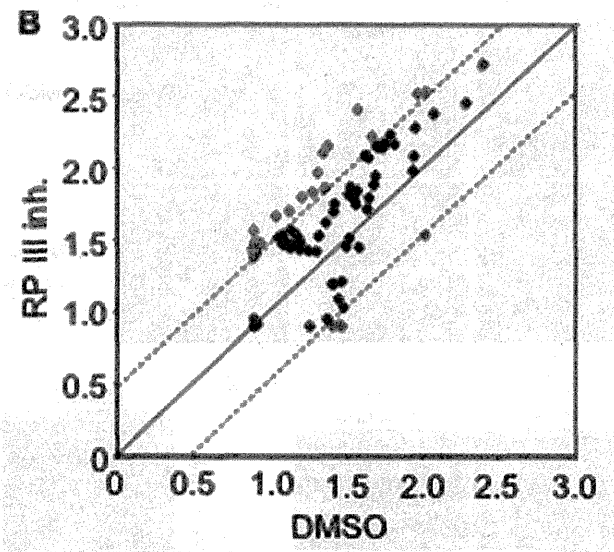


| miRNA | Fold change |
|---|---|
| miR-3162-5p | 6.82 |
| miR-92a-2-5p | 5.93 |
| miR-1909-5p | 4.51 |
| miR-764 | 3.77 |
| miR-3130-5p | 3.73 |
| miR-138-2-3p | 3.47 |
| miR-7-1-3p | 3.43 |
| miR-513a-5p | 3.25 |
| miR-181a-3p | 3.16 |
| miR-323a-5p | 3.02 |
| miR-615-5p | -3.09 |
| miR-4499 | -3.28 |
| miR-1178-5p | -3.56 |
| miR-5571-3p | -3.78 |